APPLICATION OF ON-LINE PARTIAL DISCHARGE MEASUREMENT ON ROTATING ELECTRICAL MACHINES

Major Project Report

Submitted in Partial Fulfillment of the Requirements for the Degree of

Master of Technology

In

Electrical Engineering

(Power Electronics, Machines & Drives)

By

Priya R. Nagar

(09MEE006)

Department of Electrical Engineering
Institute of Technology
NIRMA UNIVERSITY
AHMEDABAD 382 481

MAY 2011

CERTIFICATE

This is to certify that the Major Project Report entitled **"Application of On-line Partial Discharge Measurement on Rotating Electrical Machines"** submitted by **Ms. Priya R. Nagar (09MEE006)** towards the partial fulfillment of the requirements for the award of degree in Master of Technology (Electrical Engineering) in the field of Power Electronics, Machines & Drives of Nirma University is the record of work carried out by her under our supervision and guidance. The work submitted has in our opinion reached a level required for being accepted for examination. The results embodied in this major project work, to the best of our knowledge, have not been submitted to any other University or Institution for award of any degree or diploma.

Date:

Industry-Guide
Dr. S.H.Chetwani
Manager
Motors, Pumps & Engines Section
Low Voltage-Products Department
ERDA
Vadodara

Institute-Guide
Dr. S.C.Vora
Associate Professor
Department of Electrical Engineering
Institute of Technology
Nirma University
Ahmedabad

Head of Department
Department of Electrical Engineering
Institute of Technology
Nirma University
Ahmedabad

Director
Institute of Technology
Nirma University
Ahmedabad

Acknowledgements

Success of any work depends upon the dedication, sincerity and hard work. It also requires some ingredients such as motivation, guidance, encouragement and time.

I am highly grateful to Dr. S. H. Chetwani, Manager (Motors, Pumps and Engines section), ERDA, Vadodara, for his sincere advice, encouragement and continuous guidance in my work. I warmly acknowledge and express my special thanks for his inspiring discussions and infallible suggestions. I am also very grateful to Mr. R. P. Singh, Sr. Engineer, ERDA, for his valuable support through out the project.

I am very much obliged to Dr. S. C. Vora, Associate Professor, Department of Electrical Engineering, Nirma University for his inexpressible support all throughout the project.

It gives me immense pleasure to applaud Dr. M. K. Shah, Head, LV Products, Electrical Research and Development Association (ERDA), Vadodara, for providing me this fabulous opportunity to do my project work in their reputed organization.

My sincere thanks to Prof. A. S. Ranade, Head of Electrical Engineering Department, Prof. U. A. Patel, Section Head; and Prof. Dr. P. N. Tekwani, P. G. Coordinator, Department of Electrical Engineering, Nirma University for allowing me to do my project work at ERDA, Vadodara. Also I would like to thank all the other faculty members of Department of Electrical Engineering, Nirma University.

My heartfelt thank to my parents and all my friends who encouraged me and supported me throughout the course.

- Priya R. Nagar

09MEE006

Abstract

Partial discharge (PD) is a localized dielectric breakdown of a small portion of a solid or fluid electrical insulation system under high voltage stress, which does not bridge the space between two conductors. Partial discharges occur as symptoms of a number of failure mechanisms related to motors, generators and switchgear. As a result, partial discharge testing may be used as a predictive maintenance tool. For high voltage equipment, the integrity of the insulation can be confirmed by monitoring the PD activities that occur through the equipment's life. To ensure supply reliability and long-term operational sustainability, PD in high-voltage electrical equipment should be monitored closely with early warning signals for inspection and maintenance. PD can be tested by on-line or offline methods. For offline PD testing, equipment has to be disconnected from service which is not suitable for some applications. So Online PD measurement is preferred for such cases.

In this project on-line partial discharge testing is carried out on various HT rotating electrical machines. This is to find the level of deterioration in the stator insulation of the machine and to quantify the level of discharge in pC. The measurements, as done by PD measurement system, are verified with lab results. This is to ensure the suitability of application of On-line PD measurement on rotating machines. Noise causes major problem in the analysis of PD signals as they mask the original signals. So proper noise rejection technique should be used. Here various noise rejection techniques are studied and wavelet transformation technique is used for noise rejection. The results are examined and it is found that WT technique provides a robust methods for noise rejection in on-site applications where severe noise is present.

List of Figures

List of Tables

Abbreviations

HV ..... High Voltage
PD ..... Partial Discharge
HFCT ..... High Frequency Current Transformer
RFCT ..... Radio Frequency Current Transformer
TEV ..... Transient Earth Voltage
CC ..... Coupling Capacitor
PRPD ..... Phase Resolved Partial Discharge
SNR ..... Signal-Noise Ratio
VHF ..... Very High Frequency
UHF ..... Ultra High Frequency
DSO ..... Digital Storage Oscilloscope
WT ..... Wavelet Transform
DWT ..... Discrete Wavelet Transform
FFT ..... Fast Fourier Transform

Contents

Chapter 1

Introduction

1.1 Overview

Electrical systems are among the most valuable assets in any plant and can have the biggest impact on the bottom line. Their production and management cost is high, and failures almost always lead to catastrophic losses. Electrical systems are being operated at higher levels, even while systems are aging-which affects both the life and the reliability of the assets. Today's asset managers are facing the increased challenge of maximizing their aging electrical infrastructure with fewer qualified technical in-house resources, stricter regulatory requirements for worker safety, and shrinking maintenance budgets. Advances in technology, including the use of Partial Discharge Testing, are giving asset managers new approaches to achieve improved reliability and performance of critical electrical assets.

1.2 Advantages of PD Testing

Failure of High Voltage insulation is the No. 1 cause of HV system failures with IEEE statistics indicating that electrical insulation deterioration causes up to 90% of electrical failures of certain high voltage equipment. PD can be tested for high voltage equipments like Cables, Splices and Terminations, Switchgear, Power Trans-

formers and Bushings Instrument Transformers (Current Transformers and Voltage Transformers), Motors and Generators, Capacitors and Surge Arrestors. For high voltage equipment, the integrity of the insulation can be confirmed by monitoring the PD activities that occur through the equipment's life. To ensure supply reliability and long-term operational sustainability, PD in high-voltage electrical equipment should be monitored closely with early warning signals for inspection and maintenance. PD can be prevented through careful design and material selection. In critical high voltage equipment, the integrity of the insulation is confirmed using PD detection equipment during the manufacturing stage as well as periodically through the equipment's useful life. PD prevention and detection are essential to ensure reliable, long-term operation of high voltage equipment used by electric power utilities.

Industry statistics by IEEE and EPRI (Electrical Power Research Institute) indicate that approximately 40% of all air-cooled high voltage motor and generator failures occur due to failure of the stator winding insulation. Partial discharge testing will provide users with benefits such as:

1. Avoidance of unnecessary rewinds on older machines by maximizing the operating hours from a stator winding. If a rewind is not needed, the user saves on the large capital cost of such maintenance.
2. Find problems on new machines that may still be under warranty.
3. Focus maintenance efforts on machines with higher levels of PD by comparing to similar machines.
4. Increase overall safety within a plant.
5. Determining what corrective action needs to be done prior to an outage.
6. Improve the overall reliability of generators, motors and switchgears thereby reducing the risk of unexpected failure.
7. Ensuring the effectiveness of corrective maintenance. Cleaning and re-wedging are common maintenance practices for high voltage machines. After completing such work, it is important that their effectiveness be assessed. By performing a partial discharge test "before" and "after" maintenance, the effectiveness of that maintenance

can be ensured. If "after" maintenance partial discharge tests yield poor results, there might be a need to plan additional maintenance or rewind to avoid in-service failures.

1.3 Literature Survey

Literature survey plays a very important role in the project. Literature survey consists of book referred which gives fundamental knowledge of partial discharge and its testing methods. Papers were taken from IEEE conference proceedings, journal proceedings and other standard publications. IEC standards are also referred.

1 **M S Naidu and V Kamaraju, "High Voltage Engineering" 3rd edition, Tata Mc Graw-Hill, New Delhi, 2006, pp. 93-97 & pp. 379-387** [1]

   This book gives the information about fundamentals of partial discharge, discharge mechanism, types of partial discharge, terminologies related to PD phenomenon, laboratory methods for partial discharge testing, calibration procedure and PD measuring system.

2 **A.J.M. Pemen, P.C.T. van der Laan and W. De Leeuw, "Analysis and localization of spurious partial discharge activity in generator units" in proc. 2001 IEEE 7th International Conference on Solid Dielectrics, pp. 489-492**

   Paper [2] shows that, in addition to phase resolved patterns, the wave shapes of PD signals provide valuable information on the type and origin of the discharges. The complex propagation of PD signals in a stator winding is studied. It shows that a PD signal manifests itself at the generator terminals after a transit time which depends on the origin of the discharge. The amplitude of the response strongly depends on the origin of discharge. The higher frequencies are heavily damped for discharges that occur deeper into the winding, so only discharges close to the measuring terminal will be observed. Also electromagnetic couplings

in the end-winding region cause cross-talk between the phases, which depends on the origin of the discharge.

3 **Wijnand R. Rutgers, Robert Ross & Theo G.M. van Rijn, "On-line PD detection techniques for assessment of the dielectric condition of HV components" in proc. 2001 IEEE 7th International Conference on Solid Dielectrics, pp. 481-484**

The paper [3] focuses on on-line partial discharge diagnosis of HV components to provide information about the dielectric integrity during service. It states that PD patterns e.g. phase resolved PD patterns (PRPD) or time sequences of pulses (TRPD) contain information on the nature of the dielectric fault. In this paper for the on-line Pd measurements of generators two kinds of sensors i.e. rogowski coils and capacitive dividers were installed in the bus-bar near generators. Detection was optimal in the VHF frequency range between 10 and 25 MHz.

4 **Yafei Zhou, A I Gardiner, G A Mathieson, Y Qin, "New methods of partial discharge measurement for the assessment and monitoring of insulation in large machines", in proc. 1997 Electrical Insulation Conference and Electrical Manufacturing and Coil Winding Conference, pp. 111-114**

The paper [4] uses the high voltage high-frequency current transformer (HVH-FCT) for online partial discharge measurement. The CT characteristics and their applications, live-line PD calibration method for quantitative PD measurement and their performance are described. On-line PD location is described by using calibrator. It states that to avoid AM radio frequency interference, the lower frequency limit may be set above 2 MHz for high frequency PD measurement. The PD and noise signals can be distinguished by their direction of travel. A calibrator with 3.5ns rise time has been built for online calibration purpose.

5 R. Bartnikas and J. P. Novak, "Effect of overvoltage on the rise time and amplitude of partial discharge pulses", IEEE Transactions on Dielectrics and Electrical Insulation, Vol. 2, (4):557-566, 1995.

In paper [7], the effect of overvoltage on PD pulse is explained. It has been established that the form or shape of a breakdown current pulse is very much determined by the overvoltage developed across the gap. Large overvoltages lead to intense space charge effects, which appreciably modify the breakdown current pulse form, leading to more rapid rise times, greater peak current amplitudes and reduced pulse widths. In so far as the overvoltage across a given cavity affects the rise time and amplitude of the pulse resulting from a spark type discharge, the response of a conventional partial discharge pulse detector is necessarily a function of the overvoltage developed across the cavity.

6 Hutter, W., "Partial discharge detection in rotating machines", IEEE Electrical Insulation Magazine, Vol. 8, No. 3, pp. 21-32, May/June 1992.

In paper [8], off-line and on-line PD measurement of rotating machines using coupling capacitor and HCFT sensors are described. It is described that the characteristics of PD signals vary with the place of origin. Also it is given that the information required to locate partial discharges in the winding is only present in the time-related behavior of the measured signals. Risetimes, differences in propagation time, and frequency content offer information concerning the propagation of partial discharges in windings. For on-line measurements the noise suppression is achieved on the basis of time-of-arrival and high frequency attenuation.

7 Wilson, A., "Slot discharge damage in air cooled stator windings", Proceedings of the Institution of Electrical Engineers, Vol. 138A, No. 3, pp. 153-160, May 1991.

In paper [9], causes of slot discharge are discussed. It is given that the main cause of slot discharge is damage to corona screen and an air gap between the laminations and coil sides. The paper also describes the On-line testing using RFCT. Clamp-on CT is applied to cable near motor terminal with no ground on cable sheath at motor side of CT. Connection to station earth is at switchgear. Consequently, the earth return for circulating current will be at the switchgear and there will be a high frequency current imbalance between the cable conductor and sheath at the motor end. This is how CT detects PD.

8 **M. Michel B. Stewart A. Nesbitt D. Hepburn D. Guo C. Zhou, X. Zhou, "Comparison of digital filter, matched filter and wavelet transform in pd detection", International Council on Large Electric System (CIGRE), August session 2006.**

In [12], the authors experience in applying three different types of techniques, i.e. matched filter, wavelet transform and the traditional digital filter, to PD data denoising in laboratory and industrial PD testing is discussed. The results revealed that both the matched filter and WT techniques are superior to the traditional digital filters in PD detection and analysis, in terms of SNR and the number of PD pulses that can be discriminated from noise. The matched filter is the most effective when the waveform of the signal to be detected is perfectly known. It is shown that WT allows unambiguous reconstruction of the original pulse, which is extremely useful given that the distinctive shapes of PD pulses may be used to identify signal sources, for diagnosis or validation purpose.

9 **X. Song C. Zhou, D. M. Hepburn and M. Michel, "Application of denoising techniques to pd measurement utilizing UHF, HFCT, acoustic sensors and IEC 60270", 20th International Conference and Exhibition on Electricity Distribution, June 2009.**

In [13], four PD detection systems i.e. Ultra High Frequency (UHF), High Frequency Current Transformer (HFCT), Acoustic Emission (AE) sensors or

IEC60270 standard electrical contact systems are discussed. Denoising techniques such as the traditional digital filters, matched filters, discrete wavelet transforms and the second generation wavelet transforms are introduced and the most effective technique is proposed for the four PD measurement systems. It is stated that the pulsating signals originating from electronics circuits, PD signals from switchgear and those coming from underground cables can be distinguished through pulse shapes. The rise time of the PD pulses from machines may also provide information on PD location. When HFCT is used it is important to consider the denoising technique which is being applied to ensure correct reconstruction of the PD pulse shapes.

10 M. Florkowski and B. Florkowska, "Wavelet-based partial discharge image denoising", IET Generation, transmission, distribution, vol. 1, (2):3440-347, March 2007.

In [14], an application of wavelet-based denoising to phase-resolved partial discharge images is presented. The method described here is especially suited to cases in which an external additive noise uncorrelated with a partial discharge (PD) signal is present during acquisition, for example, in cables, transformers, rotating machines and gas-insulated switchgears. It is given that the fundamental issue in image recovery using wavelet denoising is the choice of the threshold value and the type of the wavelet. Wavelet-based denoising is superior to other digital filtering methods, especially in the suppression of transients, pulse-shaped and additive noise. Wavelet denoising technique provides proper shape reconstruction, hence can be used for noise denoising based upon wave-shape.

11 IEC 60034-27-2: On-line partial discharge measurements on the stator winding insulation of rotating electrical machines. (Draft Standard)

In this standard [18], nature of PD in rotating machines is given in detail. Various sources of noise and disturbances are given and also methods of noise

separation are briefly discussed. Details about PD sensors, their installation, PD measurement and measurement systems are given. Effects of machine operating factors on PD measurement are also explained.

12 G. C. Montanari and A. Cavallini, F. Puletti: "A New Approach to Partial Discharge Testing of HV Cable Systems", IEEE Electrical Insulation Magazine, Vol. 22, No. 1, January/February 2006.

In [15], the separation of PD pulses from different sources and of PD pulses from noise is based on a clustering technique that relies on a time frequency, T-W, transformation and on a Fuzzy Classification, which is applied to each recorded pulse. Pulses from different source form different clusters in T-W map. Then fuzzy logic classification is applied to this mapping tool to achieve separation of signals into classes that are homogeneous in terms of PD pulse features. These classes are sub-divided into sub-patterns showing pulse height and phase coming from a single-source type and/or location. A proper identification, to single out the type of the defect generating PD, can be achieved for each data subcluster. Thus PD noise is separated.

1.4 Objective of Project

The objective of this major project is to develop norms, procedure and verify the suitability of application of Online partial Discharges measurement on Rotating Machines like Motors and Generators by using Online PD measurement system. Also to create the core competency on the application of online PD measurement on rotating machines. It includes distinction of the PD signals from the noise signals, identifying its source and location of PD site.

1.5 Thesis Organization

Chapter 1 provides the introduction to developing need for PD testing. Advantages of PD testing are explained. It is followed by detailed literature survey. Then objective of project is defined. Finally organization of thesis is given.

In chapter 2, basics of PD and PD mechanism are discussed first. Relative advantages and disadvantages of offline and on-line methods are explained. Various off-line methods for PD measurement and their calibration process are also discussed.

Chapter 3 includes the details about the on-line PD testing using PD Testing system. The sensor options and their installation requirements are explained. Also operation steps, for on-line PD testing are described, which includes measurement steps and calibration steps. Finally diagnosis of PD pulse using PD measurement system and software are described.

In Chapter 4, different sources of noise and disturbances are given. Also various methods for noise separation are discussed. Finally Signal transfer characteristics are given.

In chapter 5, different types of PD that are present in rotating machines are given. Also PD pulse form and its propagation in windings is explained. Pulse propagation in windings, are described. Electrical pulse and RF sensing systems are briefly described. It also gives PD interpretation depending upon the pulse polarity. Effects of various machine operating factors and other environmental factors on the measurement of PD are explained in detail. Finally the noise separation techniques that are used in this project are discussed.

In chapter 6, first the comparative results of testing through lab set-up and through PD test system are given. Then experimental results are given for off-line and on-line PD testing. Inferences are given depending upon the results about the insulation condition of electrical machine. Finally the experimental results are verified with theoretical observations.

The main conclusions arising out of this project and scope for future work are

compiled in Chapter 8, which is followed by a list of references.

In Appendix A, principle PRPD patterns of various types of PD are given.

Chapter 2

What is Partial Discharge?

2.1 Introduction

According to Standard **IEC 60270: 2000** [6], Partial Discharge (PD) is a localized electrical discharge that only partially bridges the insulation between conductors and which can or cannot occur adjacent to a conductor.

PD usually begins within voids, cracks, or inclusions within a solid dielectric, at conductor-dielectric interfaces within solid or liquid dielectrics, or in bubbles within liquid dielectrics. Since discharges are limited to only a portion of the insulation, the discharges only partially bridge the distance between electrodes. PD can also occur along the boundary between different insulating materials. PD can also occur along the surface of solid insulating materials if the surface tangential electric field is high enough to cause a breakdown along the insulator surface. Partial discharges within an insulating material are usually initiated within gas-filled voids within the dielectric. These voids are generally filled with a medium of lower dielectric strength, and the dielectric constant of the medium in the voids is lower than that of the insulation. Hence the electric field strength in the voids is higher than that across the dielectric. Therefore, even under normal working voltages the field in the voids may exceed their breakdown value, and breakdown may occur [1].

There are seven types of partial discharges as shown in figure 2.1.

Internal discharges: They are discharges in cavities or voids which lie inside the volume of the dielectric or at the edges of conducting inclusions in a solid or liquid insulating media.

Surface discharges: They are discharges from the conductor located into a gas or a liquid medium and form on the surface of the solid insulation not covered by the conductor.

Corona: It is a discharge in a gas or a liquid insulation around the conductors that are away from the solid insulation.

Treeing: The spreading of spark channels during tracking, due to surface erosion, in the form of the branches of tree is called treeing.

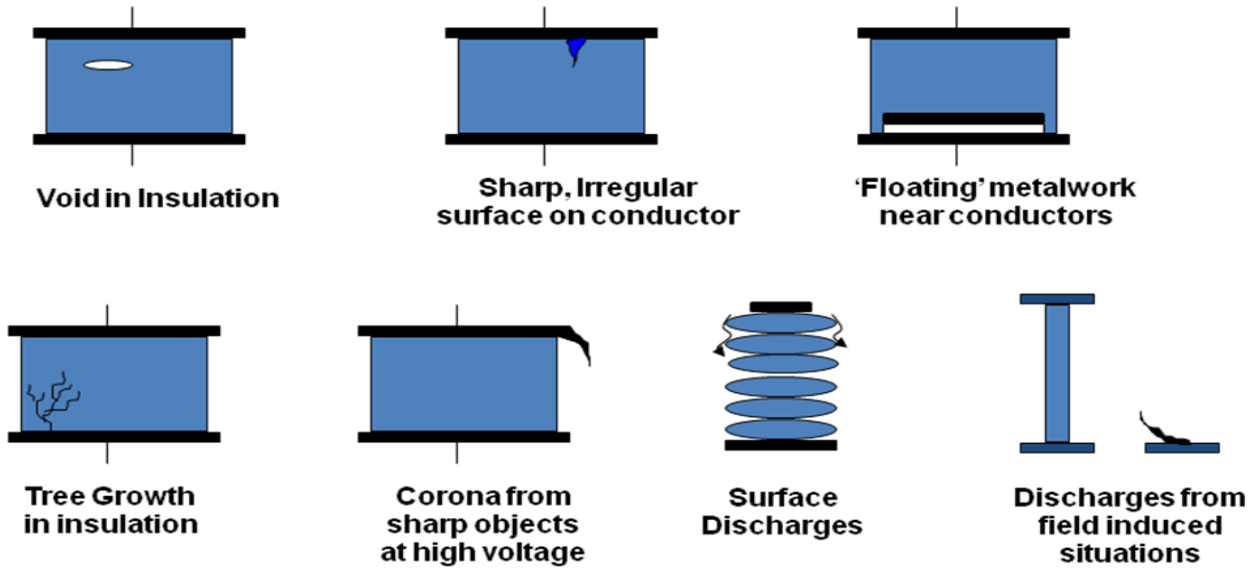

Figure 2.1: Types of PD

When partial discharge occurs energy is dissipated in various forms i.e. Electrical Charge, Optical (surface tracking and corona in air), Acoustic/Ultrasonic, Electromagnetic - RF and UHF, Ozone, Chemical by-products (such as white deposit oxides).

2.2 PD Phenomenon: Terminology Used

As per [6], following terminologies are used related to PD phenomena.

Partial discharge pulse (PD pulse): It is current or voltage pulse that results from a partial discharge occurring within the object under test. The pulse is measured using suitable detector circuits, which have been introduced into the test circuit for the purpose of the test.

Apparent charge (q): Apparent charge of a PD pulse is that charge which, if injected within a very short time between the terminals of the test object in a specified test circuit, would give the same reading on the measuring instrument as the PD current pulse itself. The apparent charge is usually expressed in picocoulombs (pC). It is not equal to the amount of charge locally involved at the site of the discharge, which cannot be measured directly.

Background noise: They are signals detected during PD tests, which do not originate in the test object.

Partial discharge inception voltage (U_i)**:** It is the applied voltage at which repetitive partial discharges are first observed in the test object, when the voltage applied to the object is gradually increased from a lower value at which no partial discharges are observed. In practice, the inception voltage U_i is the lowest applied voltage at which the magnitude of a PD pulse quantity becomes equal to or exceeds a specified low value.

Partial discharge extinction voltage (U_e)**:** It is the applied voltage at which repetitive partial discharges cease to occur in the test object, when the voltage applied to the object is gradually decreased from a higher value at which PD pulse quantities are observed.

Partial discharge measuring system: It is the system consisting of a coupling device, a transmission system and a measuring instrument.

Transfer impedance Z(f): It is measuring system characteristic, defined as ratio of the output voltage amplitude to a constant input current amplitude, as a

function of frequency f, when the input is sinusoidal.

Lower and upper limit frequencies (f_1) **and** (f_2)**:** The frequencies at which the transfer impedance Z(f) has fallen by 6 dB from the peak pass-band value.

Midband frequency fm and bandwidth Δf**:** For all kinds of measuring systems, the midband frequency is defined by:

$f_m = (f_1 + f_2)/2$ and

the bandwidth is defined by: $\Delta f = f_2 - f_1$

Pulse resolution time (Tr): It is the shortest time interval between two consecutive input pulses of very short duration, of same shape, polarity and charge magnitude for which the peak value of the resulting response will change by not more than 10 % of that for a single pulse. The pulse resolution time is in general inversely proportional to the bandwidth Δf of the measuring system.

Sensitivity: It is the magnitude of the smallest individual discharge that can be measured under particular test condition.

2.3 Discharge Mechanism

Consider a dielectric between two conductors as shown in fig.2.2. Figure shows the partial discharge within solid insulation in which when a spark jumps the gap within the gas-filled void, a small current flows in the conductors, which is attenuated by the voltage divider network C_x, C_y, C_z in parallel with the bulk capacitance C_b.

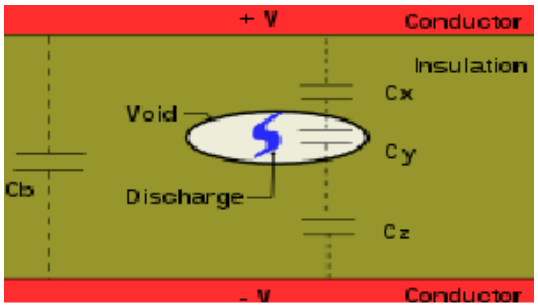

Figure 2.2: Void in Insulation

If we divide the insulation into three parts, an electrical network of C_b, C_x and C_y

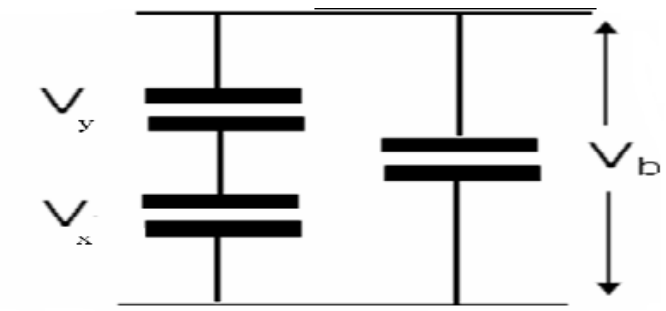

Figure 2.3: Equivalent circuit

can be formed as shown in fig. 2.3. Fig. 2.3 represents the equivalent circuit. In this C_y represents the capacitance of the void or cavity, C_x is the capacitance of the dielectric which is in series with the void, and C_b is the capacitance of the rest of the dielectric. When the applied voltage is V, the voltage across the void, V_1 is given by the equation:

$$V_1 = (V * d_1)/[d_1 + (\epsilon_0/\epsilon_1) * d_2],$$

where d_1 and d_2 are the thickness of the void and the dielectric, respectively, having permittivity ϵ_0 and ϵ_1.

When a voltage V is applied, V_1 reaches the breakdown strength of the medium in the cavity (V_i) and breakdown occurs. V_i is called the discharge inception voltage. When the applied voltage is a.c., breakdown occurs on both the half cycles and the number of discharges will depend on the applied voltage. The voltage and the discharge current waveforms are shown in fig. 2.4. When the first breakdown across the cavity occurs the voltage across it becomes zero. When once the voltage V_1 becomes zero, the spark gets extinguished and again the voltage rises till the breakdown occurs again. This process repeats again and again, and current pulses will be obtained in both the half cycles.

When the breakdown occurs in the voids, electrons and positive ions are formed. They will have sufficient energy and when they reach the void surfaces they may break the chemical bonds. Also, in each discharge there will be some heat dissipated in the cavities, and this will carbonize the surface of the voids and will cause ero-

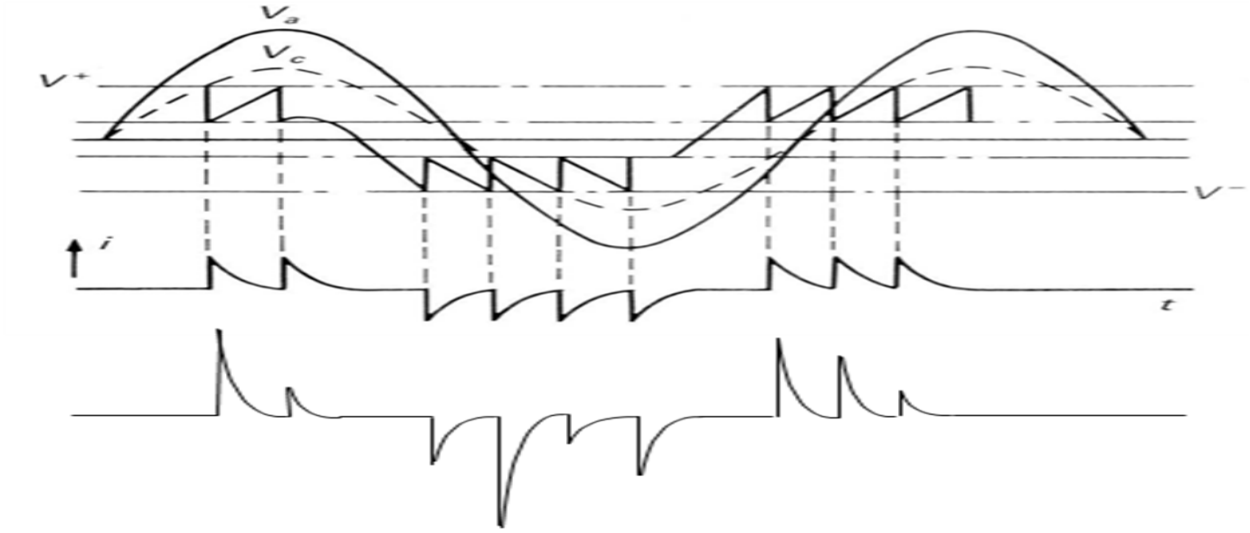

Figure 2.4: Voltage and Discharge Current Waveforms

sion of the material. Channels and pits formed on the cavity surfaces increases the conduction. Chemical degradation may also occur as a result of the active discharge products formed during breakdown. All these effects will result in a gradual erosion of the material and consequently reduction in the thickness of insulation leading to breakdown. The life of the insulation with internal discharges depends upon the applied voltage and the number of discharges [1].

For the breakdown of the gas in the cavity to occur, the discharge has to start at one end and progress to the other end. As the discharge progresses, the voltage across the cavity drops due to charge accumulation on the cavity surface towards which it is progressing, and often the discharge is extinguished. The discharge extinction voltage depends on the condition inside the cavity.

2.4 Online versus Offline PD Testing

Partial discharge testing can be done by online or offline method. For the Off-line test the equipment needs to be isolated at both ends and the portable HV power supply is applied. The move across to online PD testing over the past few years has been led by customer requests to avoid equipment outages for insulation condition testing.

Both these methods have relative merits and demerits as discussed below.

Merits of Offline PD testing:

- It's a proven technology
- Lower interference i.e. noise level due to use of Faraday Cage
- Measurement of PD inception voltage and PD extinction voltage is possible by adjusting HV power supply
- Easy localization of PD sources
- Better sensitivity than online method

Demerits of Offline PD testing:

- External power source needed
- Machine must be out of service
- Time consuming due to switching and safety requirements
- Entire winding incl. neutral end is at high voltage
- No realistic stress conditions, artificially created working condition which is applied by offline HV voltage source
- Additional PD sources are detected that are not active during actual operation.
- Expensive as outage is required
- Calibration is required before every test to ensure accurate results

Merits of Online PD testing:

- Realistic operating conditions (electric filed, current, mechanical forces, vibration, temperature)
- No need to isolate the circuit

- Economical and non-invasive
- Quick and easy to deploy, turn up, connect up and test
- Easy trending of PD activity
- Early detection of incipient insulation faults
- No external power source needed
- Testing at various load conditions
- No calibration required as sensors are calibrated

Demerits of Online PD testing:

- Data interpretation can be difficult
- Earthing pre-requisites necessary
- Considerable interference i.e. noise as faraday cage is absent
- Noise may mask actual problems
- Superposition of several PD sources
- Experience required for data analysis
- Localization of PD sources difficult

2.5 Off-line Methods

Various methods are available for offline laboratory testing of PD [1]. They are:

- Wideband PD detection circuits
- Tuned (narrow band) detection circuits
- Differential discharge bridge methods

2.5.1 Discharge Detection Using Straight Detectors

Fig. 2.5 shows the simplified circuit for PD detection. High voltage is produced using HV transformer, which is free from internal discharges. A resonant filter, Z is used to prevent any pulses starting from the capacitances of the windings and bushings of the transformer. C_a is the test object, C_k is the coupling capacitor, and Z_{mi} is detection impedance. It is a input impedance of measuring system. Measuring system consists of coupling device, transmission line and measuring instrument. CD is the coupling device, which can be a impedance box, also called as matching box. Signal developed across it is passed through a band pass filter and amplified and displayed on a CRO or counted by a pulse counter multi-channel analyzer unit. MI is measuring instrument and it comprises of amplifier, CRO, etc.

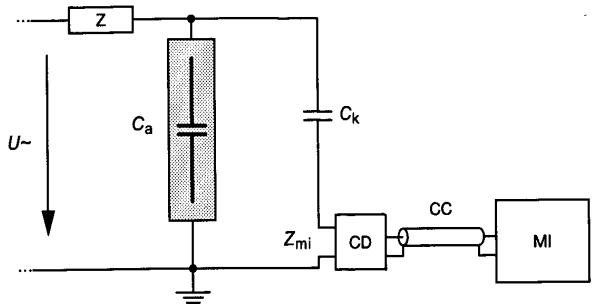

Figure 2.5: Circuit Diagram

In fig. 2.6a, the discharge pattern displayed on the CRO screen of a partial discharge detector with an elliptical display is shown. A typical discharge pattern in cavities inside the insulation is shown in fig. 2.6b. this pattern of discharge appears on the quadrants of the ellipse which correspond to the test voltage rising from zero to the maximum, either positively or negatively.

Wideband PD Detection

In the wide band detection scheme Z_{mi} is an R-C network. In combination with the coupling device, this type of instrument constitutes a wide-band PD measuring system which is characterized by a transfer impedance Z(f) having fixed values of the

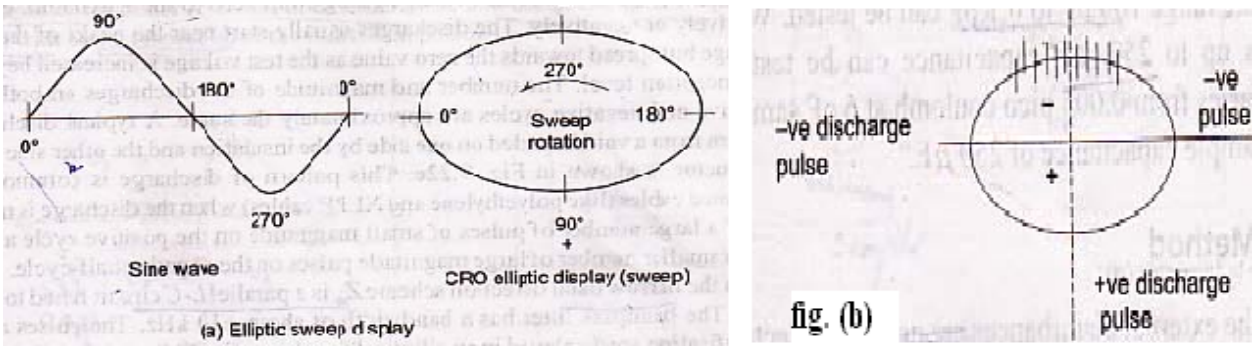

Figure 2.6: Elliptical Sweep Display and Discharge Pattern for Cavities

lower and upper limit frequencies f_1 and f_2, and adequate attenuation below f_1 and above f_2. Recommended values for f_l, f_2 and Δf are:

$$30kHz \leq f_1 \leq 100kHz$$
$$f_2 \leq 500kHz$$
$$100kHz \leq \Delta f \leq 400kHz$$

The response of these instruments to a (non-oscillating) partial discharge current pulse is in general a well-damped oscillation. Both the apparent charge q and polarity of the PD current pulse can be determined from this response. The pulse resolution time T_r is small and is typically 5 μs to 20 μs.

Tuned (Narowband) Detection

In the narrow band detection scheme impedance Z_{mi} is a parallel L-C circuit. Here narrow band instruments are used in the measuring system. These instruments are characterized by a small bandwidth Δf and a midband frequency fm, which can be varied over a wide frequency range, where the amplitude frequency spectrum of the PD current pulse is approximately constant. Recommended values for Δf and fm are:

$$9kHz \leq \Delta f \leq 30kHz$$
$$50kHz \leq f_m \leq 1MHz$$

Noise level is less in these method as bandwidth is small and noise of other frequencies are removed by narrow band pass filter. But it can be used when it is known that PD pulses will lie in that range of frequencies. The response of these instruments to a partial discharge current pulse is a transient oscillation with the positive and negative peak values of its envelope proportional to the apparent charge, independent of the polarity of this charge. The pulse resolution time Tr will be large, typically above 80 μs.

2.5.2 Balanced Detection Method

In the straight detection method, the external disturbances are not fully rejected. The filter used to block the noise sources may not be effective. The Schering Bridge employed for the tan δ measurement is sometimes used. In this method the test object is not grounded. A modification to the Schering Bridge detector is the differential discharge detector, given by Kreuger. Both the schemes are given in fig. 2.7 and fig. 2.8. The bridges are tuned and balanced at 50Hz. A filter is used across the detector terminals to block the 50 Hz components present. Signals in the range of 5 to 50 kHz are allowed to pass through the filter and amplified.

The CRO gives the display of the pulse pattern. Any external interference from outside is balanced out, and only internally generated pulses are detected. In the modified scheme, another test sample called dummy sample is used in the place of the standard capacitor. The capacitance and tan δ of the dummy sample are made approximately equal, but need not be equal. The disadvantage is that if two discharges occur in both the samples simultaneously, they cancel out, but this is very rare. The main advantage of the second method is its capacity for better rejection of external noise and use of wide frequency band with better resolution of the individual pulses.

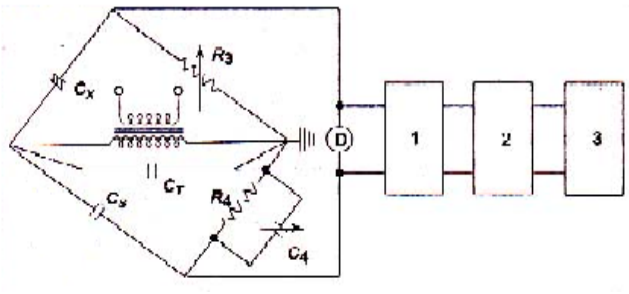

Figure 2.7: Balanced Detector using Schering Bridge

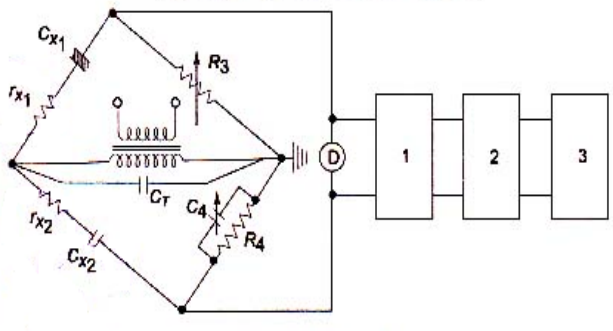

Figure 2.8: Differential Detector

2.6 Calibration

The object of calibration is to verify that the measuring system will be able to measure the specified PD magnitude correctly. The calibration of a measuring system in the complete test circuit is made to determine the scale factor k for the measurement of the apparent charge. As the capacitance C_a of the test object affects the circuit characteristics, calibration shall be made with each new test object, unless tests are made on a series of similar objects with capacitance values within 10 % of the mean values. The calibration of a measuring system in the complete test circuit is carried out by injecting short-duration current pulses of known charge magnitude q_0, into the terminals of the test object as shown in the fig.2.9.

As the capacitor C_0 of a calibrator is often a low-voltage capacitor, the calibration of the complete test arrangement is performed with the test object de-energized. For the calibration to remain valid, the calibration capacitor C_0 should not be larger than 0.l

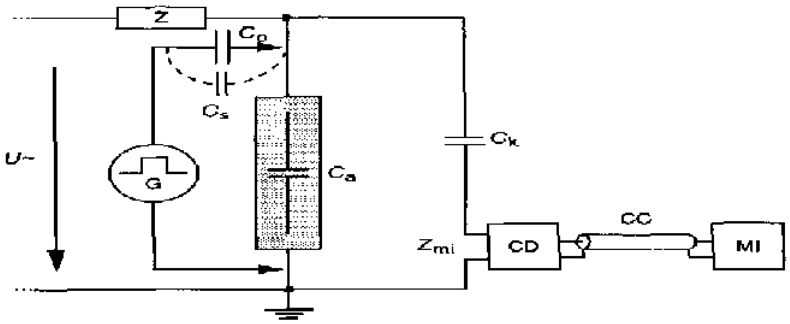

Figure 2.9: Calibration Circuit

times C_a ($0.1C_a$). If the requirements for the calibrator are met, the calibration pulse is then equivalent to a single-event discharge magnitude $q_0 = U_o \times C_o$. Consequently, C_0 must be removed before energizing the test circuit. If, however, C_o is of high voltage type, and has a sufficiently low level of background noise to allow the specified PD level to be measured at the specified test voltage, it can remain connected in the test circuit.

The current pulses are generally derived from a calibrator that comprises a generator producing step voltage pulses of amplitude U_0 in series with a capacitor C_0, so that the calibration pulses are repetitive charges each of magnitude $q_0 = U_o \times C_o$. In practice, it is not possible to produce ideal step voltage pulses. Though other waveforms having slower rise times t_r (10 % to 90 % of peak value) and finite decay times t_d (90 % to 10 % of peak value) can inject essentially the same amount of charge [6].

Chapter 3

On-line PD Testing

In this project,Partial Discharge (PD) Test Technology is used for both On-Line (in-service) PD Testing and the Off-line (Factory) PD Testing of Rotating High Voltage Machines (voltage range of 3.3kV to 17.5kV). The test system, PD sensors and the test techniques described are suitable for testing both motors and generators and most other types of HV plant. PD test kit consists of three types of sensors i.e. High Frequency Current Transformers (HFCT), Transient Earth Voltage (TEV) sensors, Coupling Capacitor. The measuring instrument used is digital storage oscilloscope (DSO). It also consists of one mini pulse generator which generates 1V source voltage used for calibration purpose. There are calibrating capacitors which along with voltagge generator produces known amount of charge, which is used for calibration purpose. The On-Line PD Testing method used by the PD test system applies a wide-band frequency measurement technique with signals collected across a wide frequency range of 40kHz to 200MHz.

3.1 Sensor Options and Installations

Making PD measurements requires some access to the PD signals which emanate from the stator winding and this is achieved by using sensors. Split-core, Ferrite HFCT sensor, TEV probes and Coupling Capacitors can either be used individually or their

combination can be used for on-line PD testing of rotating machines. Fig. 3.1 shows HFCT, TEV and Coupling Capacitor.

Figure 3.1: Types of Sensors

For larger motors and generators it is becoming increasingly common for permanent PD sensors to be fitted into the cable box of the machine. In large machines the conductors are normally carrying large load currents which has an impact on the sensors used, so Air-Cored CT's (Rogowski Coils) or High Voltage Capacitive Couplers are preferred for larger machines (10MVA+) as they do not saturate at high currents, whilst ferrite HFCTs saturate at around 1000 Amps. For smaller motors and generators it is not normally economically viable to install permanent PD sensors and thus portable, split-core inductive sensors are used to carry out On-line PD tests. As current in this case is not that large so ferrite High Frequency Current Transformers (HFCTs) can be used. Fig. 3.2 shows the positions in the machine at which these sensors are usually fitted.

HV Machines are normally directly attached to switchgear via solidly bonded cables which can often be used to measure PD activity in the machine by connecting HFCT sensors around the cable. It is recommended that the measurements are made as near to the motor as possible with short BNC co-axial cables to avoid any large signal attenuation along the measurement cables. The further you measure from the motor and the nearer measurements are made to other HV plant then the more elec-

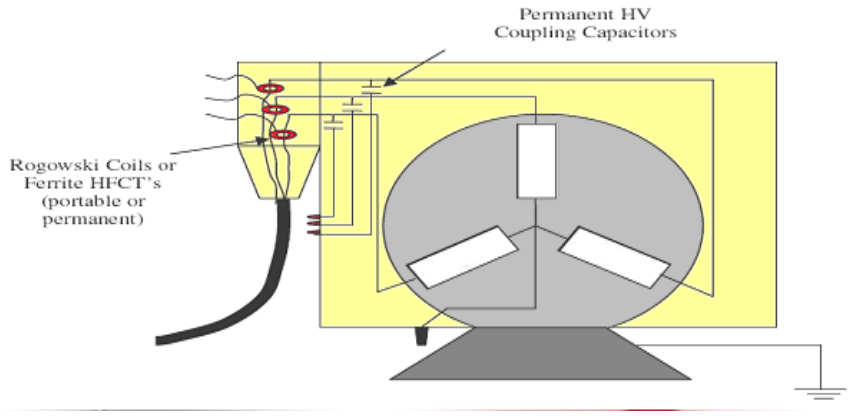

Figure 3.2: Rotating HV Machine Showing the PD Sensor Options

trical 'noise' signals will be introduced into the measurement circuit. If it is easier, or because of other constraints it is decided to work near to the switchgear end of a motor supply cable, it is considered prudent to check the signal level for attenuation and interference at both ends of the cable using the PD Spot Tester Unit before commencing on regular testing from the switchgear end of the cable. This allows the user to take into account any PD signal attenuation which may occur along the HV Cable.

In many cases it is possible to measure the PD activity in the rotating machine from the switchgear end of the cable by connecting a ferrite HFCT sensor around the earth straps or cores of the cable at the switchgear. This method picks-up the PD signals which have passed along the length of the cable from the machine to the switchgear. This method can only be used if the cable is earthed at the switchgear end of the cable only, and not the motor end. When no other access to the cable or machine windings is feasible a split-core inductive sensor (ferrite HFCT) can be connected around the earth connection of the star point of the motor but this has the limitation of combining all of the 3-phase data together.

For HV motors and generators of voltage rating 11kV and higher it is usual to have individual cables for each phase and it is thus possible to make a separate measurement for PD on each phase. With a Ferrite HFCT sensor connected around each phase of the supply cable at the motor cable box it is possible to identify discharges in-

volving both phase-to-phase insulation (end-winding discharges) and phase-to-ground insulation (slot discharges). With motors in the voltage range of 3.3 - 6.6kV it is normal to have 3-core, 'belted' supply cables and the On-Line PD test is made with the HFCT transducer fitted around all three cores of the cable. In this case the PD test unit will see only the phase-to-ground discharge pulses. Although this does not allow for the detection of phase-to-phase discharge pulses it does allow for measurement of the overall PD magnitudes as part of a 'PD Trending' analysis.

3.2 Installing Inductive Sensors

When installing the sensors around supply cables it is necessary to investigate the earth screening arrangement of the cable to ensure PD signals can be detectable. If the cable screen/armour is earthed at one point (this normally being at the switchgear) then no problems should be experienced. However, if the cable is earthed at two or more places, a reduction in sensitivity will be experienced and in extreme circumstances, no signal at all will be detectable. Multiple earthing of the supply cable sheaths can cause problems since this provides alternative paths for the high frequency PD currents to flow to the transducer. The important part about the placement of the sensor is that only the conductor current (and not the earth current) is allowed to pass through the centre of the sensor. If both the earth and conductor current pass through the sensor then it will not pick-up any signal as these two currents cancel each other out (one being positive while the other is negative and there thus being no net current through the sensor). In the case of placing the HFCT outside the cable box, then it must be ensured that the cable box is not directly earthed to the armour of the cable.

Fig.3.3 shows a suitable earthing arrangement of the cable for making PD measurements. With reference to Figure 3.3, it can be noted that in this case the cable sheath and cable gland insulates the cable armour/earth from the cable box so that no earth exists between the cable box and the cable sheath position. This means the

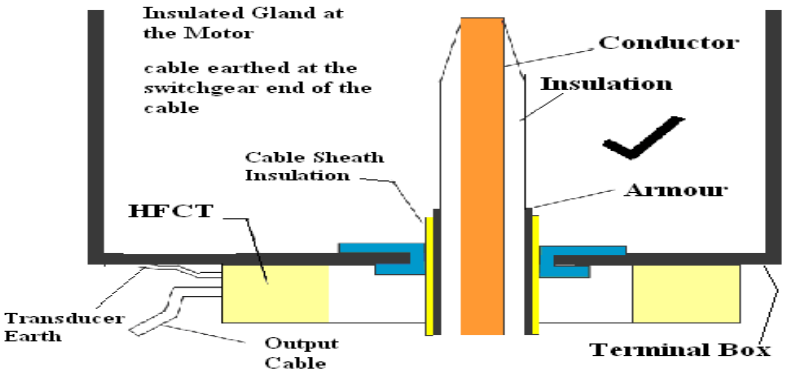

Figure 3.3: Suitable earthing arrangement for inductive sensor outside the motor cable box

PD pulses from the motor will all pass through the sensor and can thus be detected. With reference to Figure 3.4, it can be noted that in this case the cable armour/earth screen is connected directly to the earthed motor cable box. In this case the PD currents from the stator winding will be 'lost' to the motor cable box and thus PD measurements are not possible with this earthing arrangement.

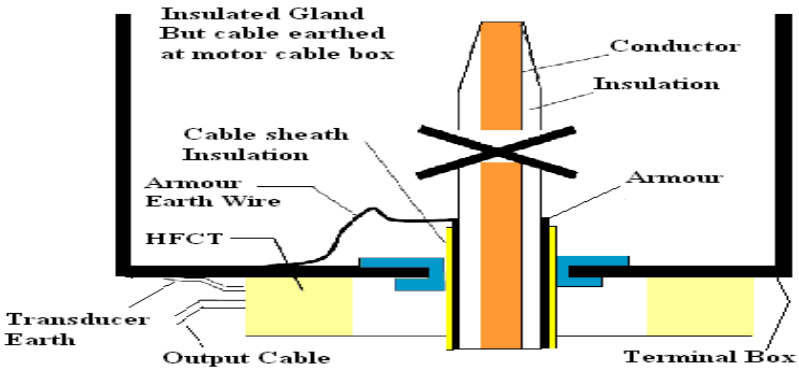

Figure 3.4: Incorrect earthing for inductive sensor PD Testing

3.3 Operation steps for PD Testing

3.3.1 Measurement Steps

Once the system has powered-up the acquisition software is started. Firstly Data Input Form is filled. All information should be filled as applicable as this is used for

initializing the measurement and is used for future references. All the parameters are set correctly on the oscilloscope for all standard measurements to ensure all signals are on-scale. After this the measurement is started and it is stored using suitable file name and location. Once the acquisition has stopped acquisition software is closed down and Reader software is opened to view the file and analysis is done.

3.3.2 Calibration Steps

For calibration purpose, calibration pulse is to be applied which should be the largest pulse on the system. Using calibrator of known value and mini pulse generator which generates 1V, known value of charge is injected into the test object. Oscilloscope is set to trigger on the channel with the calibration pulse on. Calibrator unit is connected across the HV terminal of the winding and earth. As the calibration is started the program will perform a short acquisition and ask for picoCoulomb (pC) value. The calibration constant in pC/mV will be calculated. The process should be done for the other phases also to make sure that each phase is calibrated. To make sure that the calibrations are saved it is sensible to perform a short acquisition. This can be stored at desired location and so the calibration file will saved for future use. For cases where an outage is not possible in on-line measurement, then calibrations from other similar machines can be used and loaded using file calibration. The system will remain calibrated until the calibration procedure is repeated, or the software is closed down. Remember to re-calibrate the system if the measurement method or equipment under test changes. The data from the calibration will ensure the PD test data will be recorded in pC.

3.4 Diagnosis of PD Pulse

While On-Line and Off-line Partial Discharge (PD) measurement of high voltage rotating machines is relatively easy to carry out, the diagnosis of the signals collected can be much more difficult to achieve. This is due to typically there being

numerous sources of PD from all three phases of the machine which are all measured synchronously. For the diagnostic process, using the PD Test System along with software, two levels of measurement and analysis can be carried out. They are as follows:

3.4.1 Standard Synchronous 50Hz Power Cycle Measurements

These measurements are made to show the Phase-Resolved Partial Discharge (PRPD) pattern across the power cycle. The OSM-Longshot Unit's PDGold v5.0 Software allows capturing of the signals synchronously across the 50Hz power cycle, dividing the power period into 200 slots with the peak signal detected for each slot. This allows the user to observe familiar phase-related patterns of discharge in real-time. Different types of PD activity may be present within the machine and differentiating these can be partly achieved by referencing Phase-Resolved Partial Discharge (PRPD) plots to databases of known Phase-Plot versus PD Type shapes. This is the conventional way of viewing PD data.

3.4.2 Advanced PD Pulse Waveform Measurements

This new technique uses high resolution data acquisition techniques to visualize and analyze the PD activity on a pulse-by-pulse basis. It involves the high-speed acquisition of the signals at a data acquisition rate of 100MS/s (Mega samples per second). By measuring the PD signals at such a high rate of acquisition it is possible to observe the wave shape of the PD pulses and also to measure the key characteristics of the pulses such as frequency, pulse rise time, pulse width and fall time. The high-resolution pd-pulse waveform shape data can provide information on the type and source of the PD within the rotating machine (phase-to-earth/slotdischarge, phase-to-phase end-winding discharge etc).

Chapter 4

Noise and Disturbances

An important challenge with on-line PD measurement is separating stator-winding PD from electrical noise or disturbances. In contrast to properly set-up off-line PD tests, in most online tests electrical disturbance pulses will often be present, and these disturbance pulses may be more frequent and of larger magnitude than the stator winding PD pulses, also the signals may be phase locked to the AC power frequency voltage. If the disturbances are not adequately suppressed, or the test technician is not able to adequately identify what is a disturbance and what is stator PD, there is a great risk that the disturbance will be classed as stator PD. Consequently the stator may be identified as having serious insulation problems, when in fact the insulation may be in good condition. If too many 'false positives' occur, confidence is lost in the test, and future testing may not be routinely done, losing the benefit of on-line PD testing.

4.1 Noise and Disturbance Sources

Consistent with [17], noise is defined to be non-stator winding signals that clearly are not pulses. Noise may be due to electronic devices within the PD detection system itself, for example thermal noise from semiconducting devices. Noise can also be from radio stations, radio transmitters, mobile telephones, power line carrier signals, etc.

This noise is easily separated from pulse-like signals either visually on an oscillograph display or with the use of filters.

Disturbances are electrical pulses of relatively short duration that may have many of the characteristics of stator winding PD pulses, but in fact are not stator winding PD. Some of these disturbances are synchronized to the AC cycle, and some are not. Sometimes synchronized disturbance pulses can be suppressed based on their position with respect to the AC phase angle.

Examples of **synchronized** disturbances are:

a) Partial discharges caused by e.g. electrostatic precipitators or bushing discharges

b) Power tool operation such as from arc welding and commutator sparking (may also be unsynchronized)

c) Transients caused by power electronics, for example converter fed motors or static excitation systems. This disturbance may also be unsynchronized to the AC cycle. This disturbance will be especially strong if the stator under test is fed by a voltage source converter

d) Poor electrical connections (leading to contact sparking) on the bus or cable connecting the rotating machine to the power system

e) Poor electrical connections elsewhere in the plant that lead to contact sparking

f) PD in other apparatus connected to the motor or generator terminals, for example output bus, power cable, switchgear and/or transformers

g) Arcing or sparking sources within the motor or generator, such as stator core lamination sparking

Examples of **non-synchronized** disturbances are:

h) Power tool operation (arc welding and commutator sparking)

i) Transients caused by power electronics, for example converter fed motors or static excitation systems

j) Slip ring sparking on the machine rotor

k) Overhead crane power rail sparking

All of these disturbances create electrical pulses that the unwary may confuse with stator winding PD. With disturbances d, e, f, and g, the operator normally wants to know if such activity is occurring, because it may indicate other problems (beyond stator insulation problems) that may lead to equipment failure.

4.2 Noise Separation

To reduce the risk of false indications of the stator winding insulation condition, many methods have been developed which manually and/or automatically separate stator winding PD from disturbances [18]. Many of the commercially available methods use one or more of the methods identified below.

4.2.1 Frequency domain separation

The Fourier transform of an individual PD pulse will contain frequencies from DC up to several hundred megahertz, if the PD sensor is in close proximity to the PD source. Many types of disturbances produce pulses, but the frequency content of the pulses at the PD sensor may be lower than stator winding PD. For example, sparking caused by poor electrical contacts or PD in other apparatus that is remote from the machine under test, often produce frequencies up to just a few megahertz. Thus one method of separating PD from disturbances is to use analogue or digital filters that preferentially respond to pulses in specific frequency ranges.

The PD measuring system (sensor and detection electronics) will be described as having a lower cut-off frequency and an upper cut-off frequency. Typical frequency ranges for on-line PD measuring systems are in the high frequency range (HF: 3-30 MHz), in the very high frequency range (VHF: 30 MHz to 300 MHz), or in the ultra high frequency range (UHF: 300 MHz to 3 GHz). When using measuring systems in the low frequency range (LF: below 3 MHz), the lower frequencies will be subject

to the significant influence of power line carrier, converter fed motor switching and excitation system disturbances, which need tobe suppressed.

Generally, the higher the upper cut-off frequency of the PD detection system, the greater will be the signal to noise ratio, and thus the lower will be the risk of false indications. However, the higher the lower cut-off frequency, then the lower is the likelihood of PD being detected that is remote from the sensor. However in on-line PD testing the coils near the high voltage terminal are the only ones likely to have high levels of PD activity, since the voltage is higher than for coils remote from the terminals.

4.2.2 Time domain separation

In some on-line PD monitoring systems, PD is separated from disturbances on the basis of time domain characteristics. Two types of time domain separation systems have been employed:

- Pulse shape analysis
- Time of pulse arrival

Both types can only be used with a high bandwidth detection system. Pulse shape analysis is the time domain analogy of filtering. It is predicated on specific time domain pulse characteristics such as rise-time and decay-time. Disturbance suppression using the time of pulse arrival method requires at least two PD sensors per phase to be installed on bus or cable connecting the motor or generator to the power system. This method depends on the time it takes an individual disturbance or PD pulse to travel along the power cable or bus.

4.2.3 Combination of frequency and time domain separation

Time and frequency domain characteristics can also be combined to separate disturbance pulses from stator winding PD. Time and frequency domain separation can be developed through a pulse shape analysis to produce a so-called "TF" map that plots

the equivalent timelength of the pulses versus their equivalent frequency content. The frequency content is normally calculated by a fast Fourier transform.

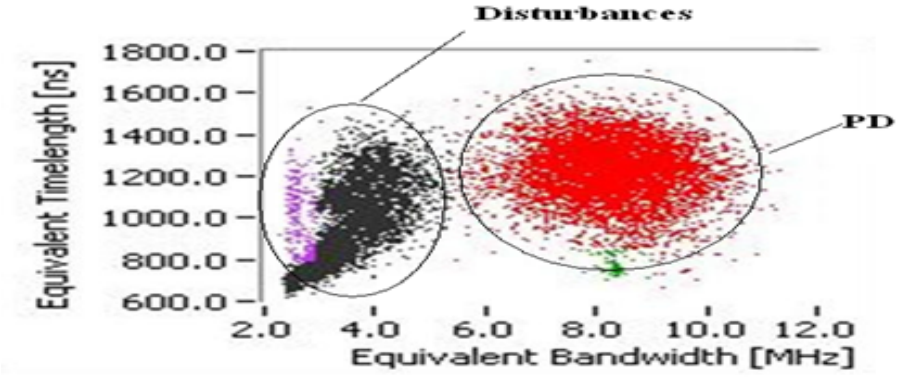

Figure 4.1: Combined time and frequency domain disturbance separation (TF-map)

In a plot of the time domain versus frequency domain characteristics according to Fig.4.1 disturbances will often appear as a cluster of pulses that is in a position, which is distinctly different from stator winding PD, and can thus be identified and suppressed from the PD pattern.

4.2.4 Gating

Certain types of disturbances such as static excitation systems (type c) produce disturbance pulses that are either phase locked to the power frequency, or the timing of the disturbances can be obtained from an external source (such as a converter fed drive). In such cases, trigger circuits can be incorporated that predict when the disturbance will occur which then will open a gate to prevent the signal from the PD sensor at the time of the disturbance from being counted as stator PD. Gating can also be used to prevent radiated disturbances from being registered as PD. An antenna can be used to detect severe radiated disturbances. The antenna signal can be processed by filters and threshold detectors to produce a gate signal whenever a disturbance in certain frequency ranges above a set threshold occurs. Since this same

radiated disturbance may also be detected by the PD sensor, the signal from the PD sensor can be interrupted whenever the gate is triggered. Some expertise is usually required to set the thresholds and since the disturbances transmission may change over time it is more appropriate for periodic monitoring systems.

4.2.5 Pattern recognition separation

Pattern recognition is the most fundamental means of separating PD from disturbance pulses. There are two basic approaches to pattern recognition: manual and automatic. In the manual method, the output of the PD sensor is displayed for example on a digital oscilloscope or a purpose built PD instrument. The display may show the positive and negative pulses, the position of the pulses on the AC cycle, as well as the magnitude of the pulses. PD pulses occur in specific parts of the AC cycle, with particular polarity relationships relative to the AC cycle. Some types of disturbances will produce pulses that occur in different parts of the AC cycle, or will appear across the entire AC cycle. In addition they may have pulse polarity relationships that may be different from stator winding PD. So stator PD can be recognized as a distinct pattern from various types of disturbances. Examples include static excitation interference (type c) that occur every 60 degrees across the AC cycle, and can easily be ignored by an observer of the display. Similarly, poor electrical contacts tend to produce pulses within a few degrees each side of the voltage zero crossings.

Automated (or computer-aided) pattern recognition is a rapidly evolving field of investigation. A number of pattern recognition methods have been applied to separate PD from disturbances and indeed separate various failure processes from one another. Some of the methods include:

- Statistical analysis of the distribution of pulses with respect to AC phase position, e.g. the mean, standard deviation of PD pulses. Stator winding PD will likely have different statistical moments than some types of disturbances
- Artificial intelligence driven pattern recognition analysis to replicate the thought

processes of an expert who manually distinguishes PD from disturbances

- Time-frequency transforms, combined with cluster recognition methods and fuzzy logic to separate and to identify pulses associated with different failure processes and types of disturbances as shown in fig. 4.2.

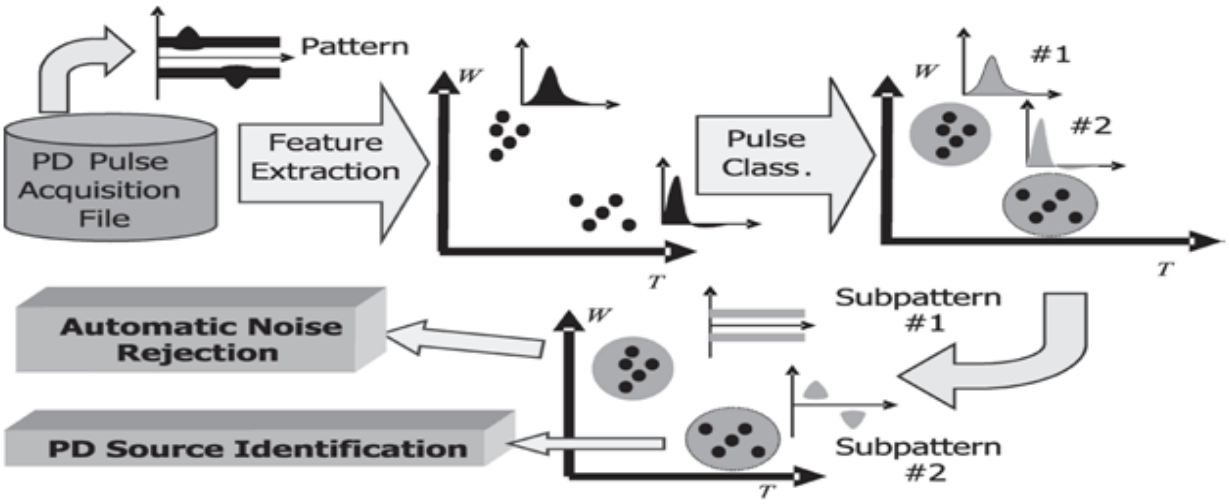

Figure 4.2: PD data processing, two superimposed phenomena consisting of DP activity and noise

As shown in fig. 4.2, here each recorded pulse is mapped in T-W plane. So pulses from different source form different clusters. Then fuzzy logic classification is applied to this mapping tool to achieve separation of signals into classes that are homogeneous in terms of PD pulse features. Eventually, typical representations, such as PD height-phase patterns, can be built up for the classes so that the acquired PD pattern can be divided in subpatterns showing pulse height and phase coming from a single-source type and/or location. Once different phenomena have been separated, a proper identification, to single out the type of the defect generating PD, can be achieved for each data subcluster. Thus PD source can be identified and noise is separated [15].

4.2.6 Wavelet Transformation

The Wavelet Transformation (WT) is a mathematical tool which has evolved from the Fourier Transform. It is particularly designed to analyze transient, irregular and non-periodic signals in a phase-space (time-scale or time-frequency) domain [12]. The WT provides a unique way of analyzing data. It presents the data in a time-scale (frequency) view, allowing the PD data to be presented in the time domain with segments of different frequency range of the data. If a wavelet can be automatically selected to match the PD pulse shape, the PD pulse could be extracted from data in any harsh environment, irrespective of the presence of any kind of noise. It involves procedure which is dependent upon the shape of the signals to be extracted from noisy environment.

4.3 Signal Transfer Characteristics

Fig. 4.3, 4.4, 4.5 shows schematically the frequency response of an idealized PD pulse at the origin of the PD within the winding (upper cut-off frequency fuPDo) and the idealized frequency response at the terminals of the machine (upper cut-off frequency fuPDt) after traveling from the PD source through the winding to the terminals. The PD measuring system, including PD sensor, measuring leads and measuring instrument, have specific lower and upper cut-off frequencies, mainly depending on the specific design of the PD sensor and the input impedance of the measuring instrument. As per [18], for PD on-line measurements on rotating machines the following typical frequency ranges for the complete PD measuring system can be defined:

A) In the low frequency (LF) range a typical bandwidth of about 1 MHz, or a few hundred kHz according to IEC 60270, is used, with lower cut-off frequencies of usually above 100 kHz and upper cut-off frequencies usually below 3 MHz. Measurement in that frequency range ensures good sensitivity not only for partial discharges in bars/coils close to the PD sensor but also for those that originate from further away

in the winding. However, the low frequency range is severely subjected to noise and disturbance. A PD measuring system working in the low frequency range basically detects the constant part of the PD pulse frequency response. So the detected PD pulses are directly proportional to the apparent charge of the PD current pulse. Since the original shape of the PD pulse arriving at the sensor location is lost when using low frequency bandpass systems, a separation of disturbance signals by pulse shape analysis or time domain separation is limited.

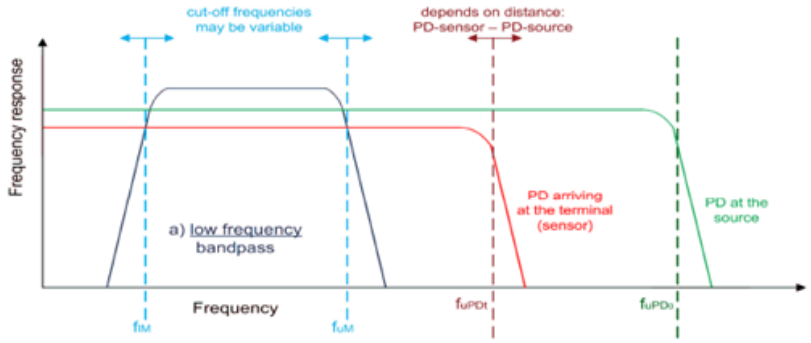

Figure 4.3: Frequency response of low frequency range PD measuring system

B) In the high frequency (HF) range a typical bandwidth of 3-30 MHz is used. PD detection in the high frequency range is less susceptible to noise and disturbance and can be efficiently used to characterize the PD pulses arriving at the PD sensor by their individual pulse shape and thus being able to discriminate between different PD sources according to their signal shape. In the case where the upper cut-off frequency of the detection system is well above the upper cut-off frequency of the PD signal arriving at the location of the PD sensor, the bandpass output signal will display the PD pulse shape but will no longer be directly proportional to the apparent charge of the PD pulse. Thus, PD results in the high frequency range are usually expressed in terms of voltage [mV]. Efficient methods of frequency and time domain disturbance separation can be applied.

C) In the very high frequency (VHF) range a typical bandwidth of a few hundred

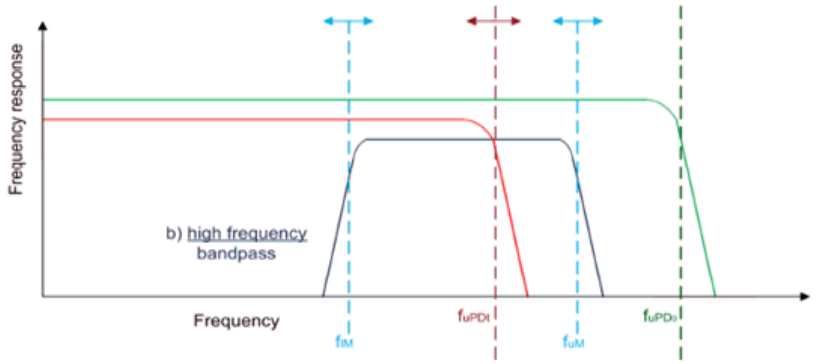

Figure 4.4: Frequency response of high frequency range PD measuring system

MHz is used with lower cut-off frequencies of typically 30 MHz and upper cut-off frequencies up to the 300 MHz range. As shown in Fig. 5 the frequency response of such systems shows a pronounced overlap with the frequency response of the original PD pulse and therefore measurements in the very high frequency range ensure a good sensitivity to signals originating closer to the PD sensor. The very high frequency range also provides a good signal to noise ratio and is therefore less susceptible to noise and disturbance. Because the upper cut-off frequency of the detection system is well above the upper cut-off frequency of the PD signal arriving at the location of the PD sensor, the measured signal will display the PD pulse shape but will no longer be directly proportional to the apparent charge of the PD pulse. Thus, PD results in the very high frequency range are usually expressed in terms of voltage [mV]. Since the shape of the original very short PD current pulse can be detected, therefore, efficient methods of time and frequency domain disturbance separation such as time-of-pulse arrival, pulse shape analysis and TF maps can be applied.

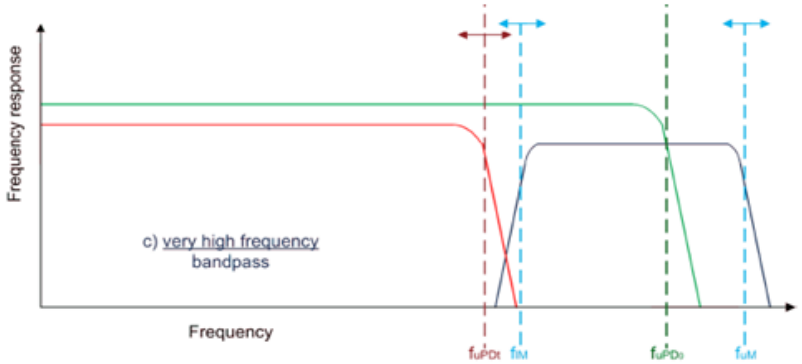

Figure 4.5: Frequency response of very high frequency range PD measuring system

Chapter 5

PD in Rotating Machines

5.1 Types of PD in rotating machine

Partial discharges may develop throughout the stator winding insulation system due to specific manufacturing technologies, manufacturing deficiencies, normal in-service ageing, or abnormal ageing. Machine design, the nature of the materials used, manufacturing methods, operating conditions, etc. can profoundly affect the quantity, location, characteristics, evolution and the significance of PD. Various types of PD are found in rotating machines [18]. They are classified as follows:

5.1.1 Internal discharges

Internal voids: Although manufacturing processes are designed to minimize internal voids, inevitably there is some void content in a resin impregnated mica tape insulation system, that is normally used in high voltage rotating machines.

Internal delamination: Internal delamination within the main insulation can be caused by imperfect curing of the insulation system during manufacturing or by mechanical or thermal over-stressing during operation.

Delamination between conductors and insulation: Thermal cycling may cause delamination at the interface of the conductor and the main insulation. This

delamination can result in partial discharges which can relatively rapidly result in failure especially in multi-turn coils.

Electrical Treeing: Electrical treeing in machine insulation is an ageing process in which fine erosion channels propagate through the epoxy around the mica barriers and may finally lead to electrical breakdown of the main insulation. Electrical treeing can start at any point of locally enhanced electric field within the insulation

5.1.2 Slot discharges

Slot discharges in high voltage machines will develop when the conductive slot portion coating is damaged due to bar/coil movement in the slot or slot exit area, for example by a loss of wedging pressure due to settlement, erosion of the material, abrasion, chemical attack or manufacturing deficiencies. Higher discharges will develop when serious mechanical damage is already present, which may result in additional damage to the main insulation and eventually in an insulation fault. Slot discharges are generally caused by locally enhanced electric fields, and thus these processes occur only at the higher voltage end of each phase.

5.1.3 End-winding discharges

Surface discharges: Surface discharges generally occur whenever the electrical field along a surface exceeds the breakdown field of the surrounding gas. This may occur if no stress control coating is applied or the stress control coating of the end-winding becomes ineffective because of poorly designed interfaces, contamination, porosity, thermal effects, etc. When reliable field grading is no longer assured, surface discharges will develop, which may gradually erode the materials.

Phase to phase discharges: PD may occur between phases, for example due to inadequate phase to phase clearances or at elements of the overhang support system like spacers or cords. Depending on specific design details these discharges may have very large magnitudes

5.2 Form of PD pulse in Rotating Machines

The form of PD intrinsic to a given discharge site will depend on the gap length, the gas and pressure within, the nature of the surface at the site between where the discharge takes place, and the statistical time lag. The product of the gap separation and the gas pressure establishes the voltage at which the PD occurs, and if the resulting discharge is of the pulse (spark) type, it also determines, in conjunction with the portion of the overall capacitance discharged, the magnitude of the PD pulse. The statistical time lag represents the time necessary for a free electron to appear within the gap, once the applied voltage across the gap attains a value equal to the breakdown value. If the appearance of the free electron is delayed, the breakdown event is initiated at some value of voltage in excess of the nominal breakdown voltage.

The difference between the actual breakdown voltage and the nominal breakdown voltage of the gap is commonly referred to as the overvoltage across the gap. The larger the overvoltage, the more intense becomes the space charge field developed adjacent to the cathode; this leads to pronounced secondary electron emission at the cathode caused by photon impact, resulting in rapid (fast rise-time) pulses having high amplitudes. The larger the overvoltage, larger is the pulse amplitude and the shorter is its rise time [7]. At large overvoltage, the detected discharge pulse current consists almost entirely of the electron current component; whereas, at zero or low overvoltage, the more protracted discharge current pulses, show an ion current component tail due to the slower moving ions [11].

5.3 Pulse Propagation in Windings

The response of a particular stator winding to a PD pulse varies depending on the length of the stator core, whether the winding is of the multi-turn coil or single-turn, the end arm geometry and the insulating materials involved. In addition, the PD pulse rise time and its pulse width will be factors in the response of a given detection

system applied to a particular winding. So it can be said that the frequency response of the detection system will profoundly influence the characteristics of the signal detected at the terminals of the stator winding.

Wide-band pulse response tests on stator windings have shown that a fast rise-time pulse is capacitively coupled through the winding, and this is followed by a slower electromagnetic traveling wave. In many windings, the fast rise-time, capacitively coupled pulse is subjected to rapid attenuation. Generally, the conventional models developed to treat pulse propagation are not applicable at the frequencies (>100 MHz) implied by this type of coupling.

Concerning the slower, electromagnetic traveling wave, the stator winding is treated as a transmission line, with each coil or bar having an associated inductance or capacitance. Depending on the length of each coil or bar and the number in each parallel circuit, every winding will possess a unique set of resonant frequencies. If the pass band of the sensor/detector system coincides with one of these frequencies, the magnitude of the measured PD will be abnormally high.

Pulse propagation problems are further compounded as the consequence of the overhang region where the coils/bars make the transition from core iron to free space and back to core iron. The surge impedance of a typical stator bar has been found to be in the range of 20-30 Ω, whereas in the end arm area, the surge impedance is higher (approximately 300 Ω) but not well defined. Thus, a PD pulse traveling along a stator bar will experience a reflection at the end of the slot, whereas in the end arm area, the transmitted pulse will be further reduced in magnitude because of cross-coupling with other circuits. Cross-coupling can be a source of errors in measurements on the other circuits.

The above factors should be considered when selecting an appropriate coupling device. PD detection systems operating above 30 MHz can benefit from the attenuation of noise signals and provide for cancelation of noise pulses based on time of arrival. Such a system is sensitive primarily to PD in bars and coils near the coupler. For off-line tests on complete windings, noise levels are generally low, and therefore,

it is preferable that such measurements be made at frequencies below 500 kHz to improve the response of the detection system to PD sources remote from the terminals. The main disadvantage of PD measurements on windings at these lower frequencies, other than the previously noted resonance problems, is that of pulse superposition, in which anomalously high PD levels may be measured if the pulse repetition rate is comparable to the bandwidth of the detector [11].

5.4 Electrical Pulse and RF Radiation Sensing System

When a PD event occurs at some location in a winding, the injected charge first flows into the capacitance to ground at the injection site, thereby modifying the local voltage. This voltage change immediately becomes the crest of a wave that propagates in both directions away from the injection site. The nature of the wave at any location away from the injection site depends entirely on the impedance along the path it had to traverse. This electrical PD pulse is captured by the sensors and it is given to measuring instruments where the pulse is measured and analysis is done. Various sensors and measuring units are available for on-line, off-line PD testing as per [11]. Here some typical systems for on-line PD measurement are discussed.

1. Using RFCT (Radio Frequency Current Transformer), HFCT and Coupling Capacitor

A 10nF capacitive coupler with broadband HFCT at line terminals and RFCT with or without 10nF capacitor between machine neutral and ground as shown in fig. 5.1 [8].

The measuring instrument does narrow-band and broadband data acquisition in time and frequency domain. The frequency range of the system is around 10 kHz to 30MHz. Here noise rejection is achieved based on time-of-arrival or high frequency attenuation. A signal imposed from the power system or generated in a phase other

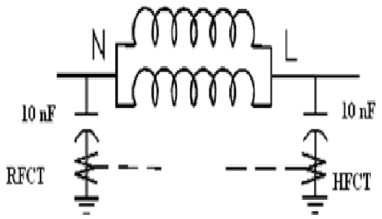

Figure 5.1: Connection Diagram

than the two phases being monitored arrives at the same time at the two sensors and can be canceled using a differential amplifier. A signal generated in one or the other phase being monitored arrives at different times at the two capacitive couplers and generates a signal at the output of the differential amplifier. Algorithms have been developed to detect phase stable disturbances with amplitudes in the range of, or greater than, PD signals prior to the PD test. The phase stable disturbances can then be eliminated with time domain gating i.e. dividing the PD measurements into as many phase windows as necessary to isolate the phase-stable disturbances. Frequency stable disturbances are removed digitally, using adaptive filters. It is applicable to motors, generators, synchronous condensers.

2. Using Clamp-on CT

Clamp-on CT applied to cable near motor terminal with no ground on cable sheath at motor side of CT. [9]

The measurement system have discharge detector with CRT display. Its frequency

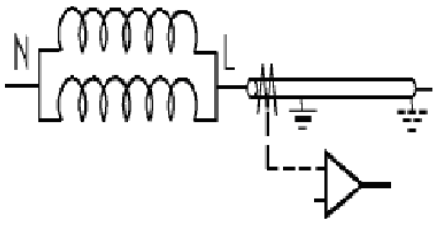

Figure 5.2: Connection Diagram

range is 50-300 kHz. It relies on there being no noise. It is applicable for motors only [11]. Large auxiliary motors on a modern station are connected to remote switchgear

using single-phase extruded power cable. The cables act as the capacitive source for compensating current for any discharge voltage pulse reaching the motor supply terminals. To avoid power frequency circulating currents, the practice is to have single bond-earthing, with the connection to station earth being at the switchgear. Consequently, the earth return for this current will be at the switchgear and there will be a high frequency current imbalance between the cable conductor and sheath at the motor end. It is this which is detected using the current transformer.

3. Using RFCT and Surge Capacitor

RFCT can be connected on the ground lead of surge capacitor applied to motor terminal as shown in fig. 5.3 [11].

The measurement instrument used is pulse height analyzer possibly with pulse-

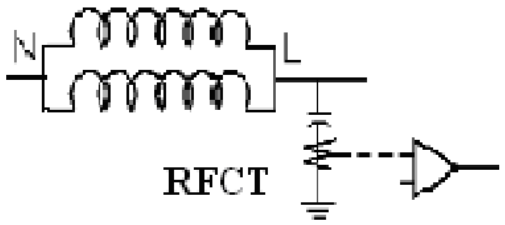

Figure 5.3: Connection Diagram

phase capability. Frequency range is 100 kHz-30 MHz for sensor and 20-350 MHz for detector. For noise rejection it relies on there being no noise, or that external noise is attenuated by cables at the frequency of measurement. Here surge capacitors are required and also this system is vulnerable to external & internal noise if present.

4. Using RFCT

RFCT is connected between generator neutral and grounding transformer as shown in fig. 5.4 [10]. Arcing is a symptom associated with copper conductor fatigue failure. The resulting arcs cause RF currents to flow through the stator winding. Measurement of RF currents that flow through the stator winding can be done using radio noise meters. The frequency range is 20 kHz-50MHz. Here noise rejection is based on manual analysis of data across the frequency spectrum. This system does not

discriminate between PD occurring on the positive and negative half-cycles of 50Hz.

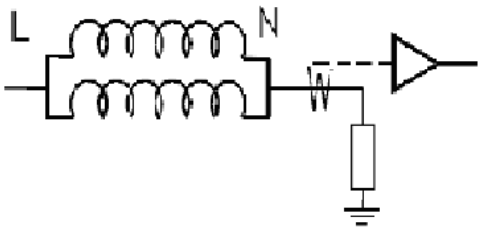

Figure 5.4: Connection Diagram

5.5 PD Interpretation Using Pulse Polarity

Inspection of the phase resolved plots reveals the phase angle relationship between the PD pulse and the phase-to-ground reference voltage. PD that originates within the slot portion of the coil, internal, is centered near 45 of the AC cycle for negative pulses and 225 for positive pulses. This is the classic position for pulses dependent upon phase-to-ground voltage levels of the specific phase being measured. Phase-to-ground voltage stresses occur all along coils within the length of the slots in the stator iron. Hence, this type of display is indicative of PD occurring in the slot and is sometimes referred to as slot-based PD. The polarity of the classic pulses and their predominance tells a lot about the relevant failure mechanism as shown in Fig. 6.10. Due to space charge effects, a pulse will occur in a specific direction based on the proximity of the void to a metallic substance. For this reason, it is possible to determine where the pulses originate, and therefore, the location of the voids in the insulation system. Several failure mechanisms produce voids predominantly at a certain location in the insulation. By observing the pulse polarity it is often possible to determine which failure mechanism is dominant.

As shown in the fig. 6.10, if positive PD activity is more as compared to negative PD then void is present in the space between insulation surface and iron core. Similarly if negative PD activity is more than positive PD activity then void is at interface of

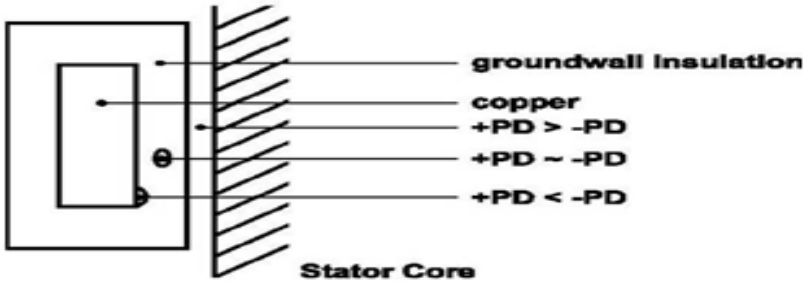

Figure 5.5: PD Polarity based on Void Position

copper and insulation. If positive and negative PD activities are approximately equal then void is present in the bulk of insulation [19].

5.6 Effect of Machine Operating Factors

The information on the likely deterioration mechanism can be obtained by analyzing the effect of various machine operating factors. Particularly the influence of load and temperature on the specific PD behavior can be efficiently used to identify typical deterioration mechanisms resulting in stator winding PD [5],[18].

5.6.1 Steady load conditions

The main machine operating factors that influence the PD behavior are:

a) Load conditions: The load conditions of the machine given as active and reactive load are characterized by the actual stator current, the stator voltage and the power factor. These parameters directly determine the winding and core temperature of the machine as well as the electrical and mechanical stresses on the stator winding insulation system.

b) Machine operation mode: The operation mode of a machine, which may be operated in peak or base load, may have an influence on the ageing behavior of the stator winding insulation system due to thermal and mechanical stresses.

c) Cooling system: Depending on the rated machine power different cooling systems are used. The stator winding may be direct or indirect air- or hydrogen-cooled or even direct water-cooled. The different cooling methods and type dependent designs significantly influence the thermo-mechanical stress of the stator winding components. In addition, for gas cooled machines, the cooling gas pressure influences the PD activity.

d) Effect of Operating Voltage: In [5], database was prepared and analyzed to determine the effect on Qm (Peak apparent charge) of operating voltage, rated power and winding age. Table 6.4 shows the average and various percentiles of Qm distribution measured by 80 pF capacitors on the stator terminals of air-cooled stators operating from 2 kV to 15 kV. As the operating voltage increases, there is a marked increase in the average and 90% Qm measured. Not unexpectedly, the operating voltage has a significant impact on the Qm. At higher operating voltages, a higher Qm is expected. In correlations with observed winding condition, it is that if the Qm is higher than the 90% level in the database for the same voltage class, then significant insulation deterioration will be observed in a winding. From Table 5.1 it is clear that significant insulation deterioration occurs with a Qm of about 514 mV for a 13.8 kV stator, while the same level of deterioration in a 6.9 kV motor occurs about 220 mV. Thus the operating voltage has an important impact on how a particular Qm should be interpreted. Clearly results from a 13.8 kV stator should not be confused with those from a 6.9 kV stator.

Table 5.1: Distribution of Qm for Air-cooled Stators, 80pF sensors on the terminals

Oper. Volts	*2-4kV*	*6-8kV*	*10-12kV*	*13-15kV*
25%	5mV	13mV	36mV	37mV
50%	22	37	83	96
75%	73	112	207	236
90%	155	218	473	514
Average	91	86	193	212
Max. Recorded	3200	1805	4455	4127

e) Power Rating: Similar analysis was done for the other factors previously listed. The analysis showed that the distribution of Qm did not depend on the power rating of the motor, as long as the voltage class, type of sensor and type of cooling/pressure was held constant. That is, the 90% Qm level is the same for a 1,000 HP and a 10,000 HP motor, as long as the voltage class, etc is the same.

f) Winding Age: Also there is no consistent trend - which is surprising since one would normally think older windings would be more deteriorated and thus have higher PD levels. Results show that there was no general trend which implies that both older windings and new windings can have about the same high PD activity. In fact, air-cooled motors manufactured in the past 5 years seem to have higher PD activity than some of older machines. This may reflect the fact that modern windings tend to operate at higher thermal and electrical stresses than older machines.

g) Ambient conditions: The main ambient influence factors on the PD behavior of the machine are humidity and particularly contamination, like partly conductive grease, dust, oil etc., which may for example occur in open-circuit air-cooled machines. Due to these influencing factors, for the analysis of the PD behavior in correlation to the machine operating conditions, it is recommended to record the operating parameters.

5.6.2 Transient load conditions

Variations of the PD trend parameters and/or the PD patterns with respect to operating parameters can assist in identifying the source of PD and its relative severity. Some new windings may require several months of operation before stable "benchmark" readings are possible because of the continued cure of resin and slot contact effects.

a) Change with load: When temperature and voltage are held constant, a change of the PD magnitudes within the negative voltage half-wave between low load and high load is indicative of a loose winding. This effect is due to stronger

electromagnetic forces acting on the winding at higher load. Such signs merit early investigation because erosion of thermosetting groundwall insulation caused by the combination of slot discharge and electromechanically induced vibration can be rapid.

b) Change with power factor: When temperature and voltage are held constant, a change of the power factor allows distinguishing between PD caused by high electric fields and arcing effects due to electromagnetic current forces. This can be identified with the ϕ-q-n pattern since in contrast to PD resulting from high electric fields, arcing effects driven by electromagnetic forces lead to typical phase shifts of PD pulses within the discharge pattern.

c) Change with temperature: When load and voltage are held constant, a change of the PD magnitudes as the temperature increases or decreases is usually indicative of discharges mainly resulting from the slot portion of the winding. This may be a sign of delaminations between inner conductor and insulation or between layers of the main insulation or even a sign of slot discharges. The influence of temperature changes on the behavior of PD from the end-winding region can hardly be assessed.

d) Change with gas pressure: In the case of hydrogen-cooled machines, there may be an opportunity to make PD measurements at different gas pressures. These results can be useful in confirming the sources of PD. Especially surfaces discharges will be more prominent at low gas pressure. When decreasing the gas pressure, caution is needed in particular for aged stator winding insulations, since the loss of external gas pressure may lead to mechanical overstressing of the insulation due to the still existing internal gas pressure in voids and delaminations.

e) Change with humidity: The humidity of the surrounding cooling gas will have an effect on the behavior of surface discharges. Lower PD has been attributed to the surfaces of the end arms at times when the humidity is high because of a homogeneous field grading effect on the winding surface. However, in the presence of severe contamination higher humidity may result in local conductive paths that lead to additional surface discharges.

5.7 Noise Rejection Techniques Applied

The PD measurement system which is considered in this project mainly utilizes wavelet denoising technique for the purpose of noise separation and signal identification. The system is also based on frequency domain separation and pulse shape analysis (time domain separation) for separating noise signals from machine PD signals. The mother wavelet of order 4 is selected for wavelet transformation. The system also provides with phase resolved partial discharge plots. These PRPD plots can be compared with the well-defined, standard PRPD plots as given in appendix A. Thus manual pattern recognition separation method can also be applied for noise separation and also identifying the type of PD source. Due to high speed data acquisition of signals, signal characteristics are also available. So depending upon rise time, fall time of the signal the PD signals can be separated from noise signals. The FFT of the signals, captured, is carried out and depending upon signal frequency the PD signals are segregated. The sensors used has frequency response in high frequency range (3-30MHz). So methods of noise rejection in time and frequency domain can be applied. But the output of the sensors is not proportional to the apparent charge of the discharge. Hence PD value in mV is given.

5.7.1 Wavelet Transformation Technique

The block diagram in Fig. 5.6 shows the scheme of the general DWT, where the filter pair h$\sim$ and g$\sim$, low-pass and high-pass respectively, are adopted from a Mother wavelet. When a signal is decomposed, at each level of DWT, the signal is passed through a low-pass filter and a high-pass filter to characterize the low and high-frequency contents in the signal, which are characterized by the wavelet coefficients. The coefficients representing the low-frequency contents are known as the signals "approximations" and the coefficients representing the high-frequency contents are known as its "details". The approximations of the signal keep the global feature content of a signal under examination, whereas the details tell us the irregular and

transient contents of a signal under analysis. When DWT is applied in PD measurement denoising, the process involves DWT decomposition, thresholding and signal reconstruction via Inverse DWT [16].

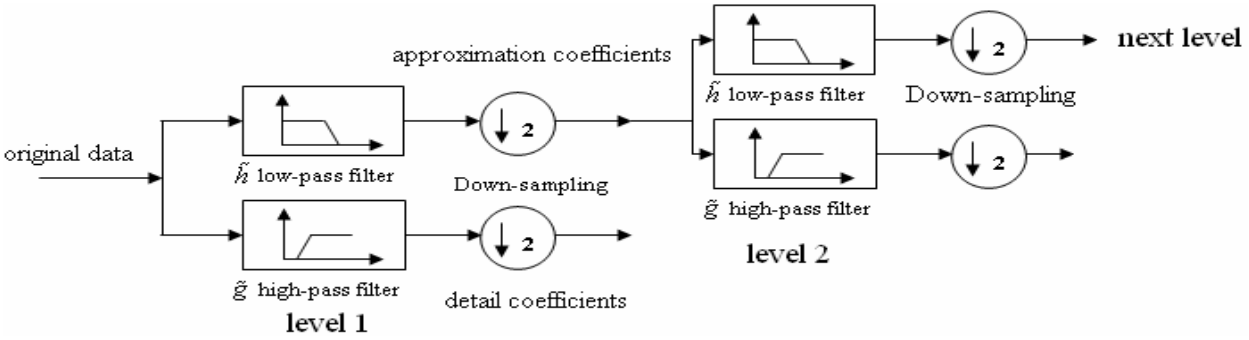

Figure 5.6: Discrete wavelet transform: filtering and down-sampling

Wavelet signal decomposition results in a set of wavelet coefficients that can be considered in two dimensions, one being time and the other being the scale or level of the wavelet. This latter parameter relates to scaling of the wavelet to change its effective frequency band and, thus, the various levels can be associated with frequency bands. Thus the wavelet transform characterizes the signal in both time and frequency. Wavelet-based denoising depends on selecting a wavelet that matches well the shape of the transient signal to be extracted from the noise. This results in large wavelet coefficients at just a few levels (or scales), which are associated with the desired signals, while noise is more widely spread among the levels. Denoising can therefore be effected by reconstructing the signal after eliminating the coefficients associated with noise while preserving those closely associated with the desired signal.

The PD waveform, depending on the physical mechanism, transmission path in the insulating system and detection mode, can generally resemble either unipolar, exponential like-shape or oscillating pulse as shown in Fig. 5.7 [16]. Transient, aperiodic signals, such as partial discharge, are best extracted with an asymmetrical wavelet basis function, which provides a better match to the shape of the PD pulse than does a symmetrical waveform. The Daubechies wavelets meet this criteria. Fig.

5.8 and Fig. 5.9 shows the shape of Daubechies wavelets db2, db4 and db8, where the number behind the wavelet name stands for the wavelet order. As can be seen from Fig. 5.7, 5.8 and 5.9, the shape of the Daubechies wavelets matches that of the PD pulses very well. The first class of PD pulses can be well approximated with db2 mother wavelets, whereas for the latter one, the higher order mother wavelets are used. As we go to higher order of wavelets, the waveform of wavelet becomes more oscillating. If the mother wavelet of different order is selected, then accordingly the number of PD events, that are recognized has PD, also changes to some extent. Also depending upon level of thresholding used number of PD events extracted changes. Thus wavelet transformation provides robust technique for noise separation.

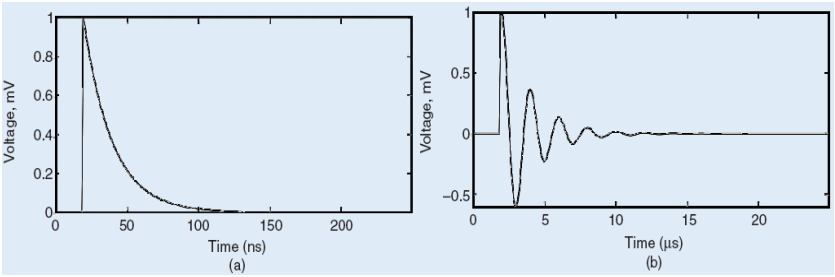

Figure 5.7: Typical PD pulse shapes

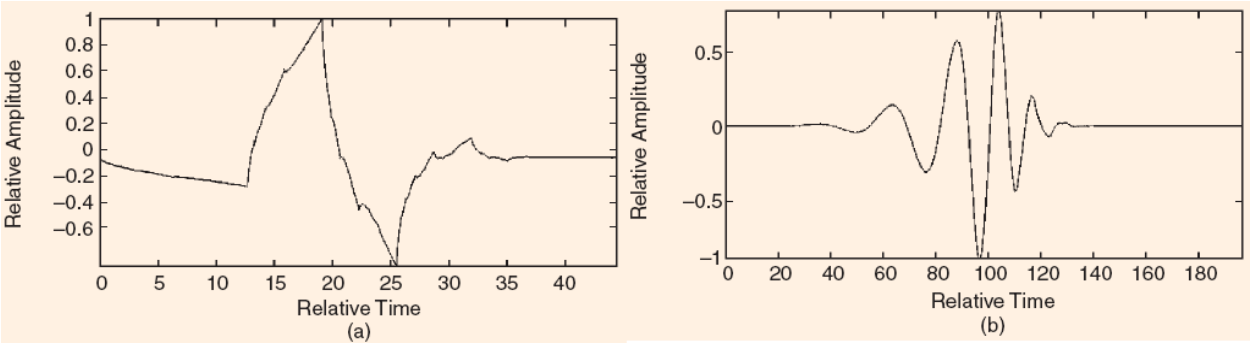

Figure 5.8: Waveforms of Daubechies wavelets, (a) db2 wavelet and (b) db8 wavelet

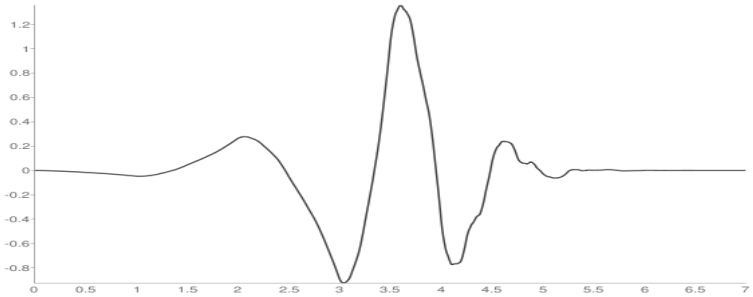

Figure 5.9: Waveform of Daubechies wavelet, db4

5.7.2 Pulse Shape Analysis

Pulse shape analysis is the time domain analogy of filtering. It is predicated on specific time domain pulse characteristics such as rise-time and decay-time. For example, a PD sensor located close the source of the stator PD may result in a detected rise-time that is shorter than a specific time, whereas certain kinds of disturbances as mentioned earlier may be characterized by a longer rise-time. Digital circuits can separate stator PD from such disturbance sources by measuring the rise-time. Generally, the further the PD or disturbance source is from the PD sensor, the longer will be the rise-time of the detected pulse, since series inductance and/or the traveling wave phenomena called dispersion (frequency dependent velocity) tends to suppress the higher frequency components of a pulse. As per [11], the PD signals have their rise-time in the range of few nanoseconds. Thus with the help of rise-time, fall-time characteristics the PD signals can be recognized.

Chapter 6

Experimental Results

6.1 Verification with Lab Results

PD Testing was done on 66kV cable using laboratory set-up and the PD measuring system used in the project at different test voltages of 12, 15 and 16kV. Table 6.1 gives the comparative results of lab and PD measuring system. As seen from the table, the results are matching. Thus it can be said that this system can be used for on-line PD measurement of rotating machines.

Table 6.1: Comparison of Lab Set-up and PD Test System

Test Voltage (kV)	*Lab. Results (pC)*	*PD Test System Results (pC)*
12	approx. 2000	2310
15	approx. 6000	6217
16	approx. 8000	7948

PD Testing was also done on 33kV CT using laboratory set-up and the PD measuring system at test voltages of 5kv, 10kV and 12kV. PD inception took place at 12kV. PD value obtained by lab. set-up was around 2000pC and that obtained by PD test system was 2150pC (using Coupling Capacitor) and 1230pC (using HFCT). Thus results matched with lab. results.

6.2 On-line PD Testing ♯ 1

On-line partial discharge testing was done on three phase, 50Hz, 6.6kV HT motor. Partial discharge within the insulation system of HV Motor is measured using three HFCT (High Frequency CT) sensors and one TEV (Transient Earth Voltage) probe. The HFCT sensors were clamped on the line side of each of the three phases of the motor and TEV probe was placed on the outer body of the terminal box. The test set-up is as shown in the figure 6.1.

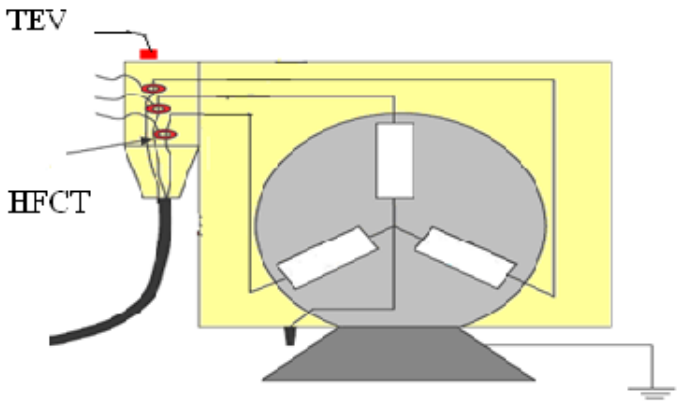

Figure 6.1: Test Set-up

The HFCT sensors are placed as close as possible to the terminals. These sensors are connected to the DSO of PD measurement system on the other side. DSO has four channels. HFCT sensors clamped on R, Y and B phase are connected to channel 1, 2 and 3 respectively. TEV probe is connected to channel 4. Figure 6.2 shows Peak PD magnitude of all the four channels with respect to time. Fig. 6.3 shows the PD data of all the channels across the power cycle.

Table 6.2 shows the peak value of PD events in all the 4 channels, both in mV and pC.

Fig. 6.4 shows machine PD across power cycle and segment waveform of highest PD event of R phase. The signals are captured at the sampling rate of 100MS/sec. For each acquisition 5 cycles are captured. The width of each PD segment waveform is 15sec. As shown in the fig. 6.4, there is only one PD event identified in phase

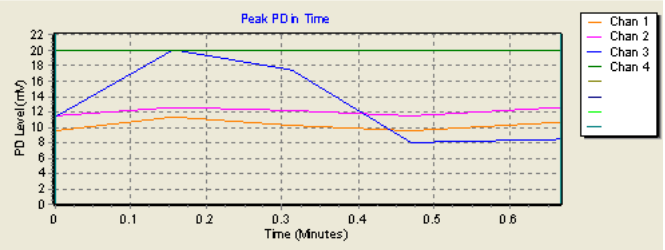

Figure 6.2: Peak amplitude v/s Time

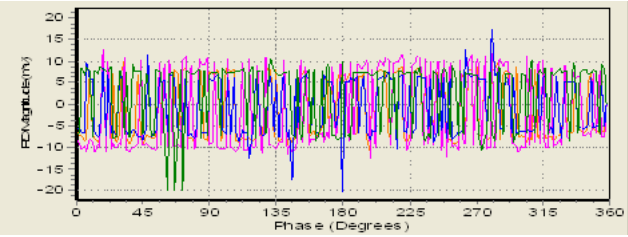

Figure 6.3: Cumulative PD Data

R. All the other signals captured by channel 1 are either noise signals or switchgear PD signals. The value of highest waveform segment is -7.72 mV which is equivalent to -170.39 pC. Its rise-time is 87.89 nSec and fall time is 57.76 nSec. Frequency of maximum amplitude is 3.96 MHz. Fig. 6.5 shows noise signals of phase R and segment waveform of highest signal.

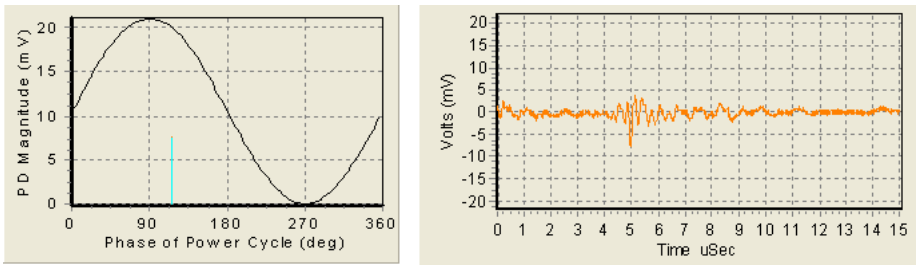

Figure 6.4: Machine PD and Segment Waveform

Also no considerable PD is identified in phase Y. All the signals captured are noise signals. Figure 6.6 shows noise events of phase Y and the segment waveform of highest noise signal. Considerable PD is identified in phase B i.e. total 14 machine PD events are identified. The machine PD of phase B and segment waveform of highest PD event is shown in fig. 6.7. Its value is -20.16 mV, which corresponds to -802.10 pC. Its rise-time is 54.31 nSec. Frequency of maximum amplitude is 1.2 MHz.

Table 6.2: Peak PD Level

Sensor	*Position*	*Peak Value in mV*	*PD Level in pC*
HFCT	R-phase	-7.72	-170.39
HFCT	Y-phase	low	low
HFCT	B-phase	-20.16	-802.10
TEV probe	Terminal Box	-20	26.02dB

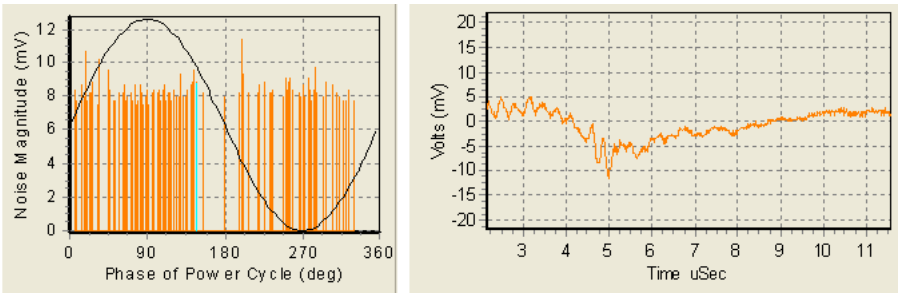

Figure 6.5: Noise Events and Segment Waveform of Phase R

HFCT gives output in mV and depending upon its transfer impedance, the value of PD current in mA can be obtained. By integrating this current value, PD value in pC can be obtained. pC value depends upon rise time, fall time, amplitude of PD signal. If the signal travels more distance between its origin and sensor location, then signal rise-time and fall time increases and amplitude decreases. This changes the value of signal pC as given by the sensor.

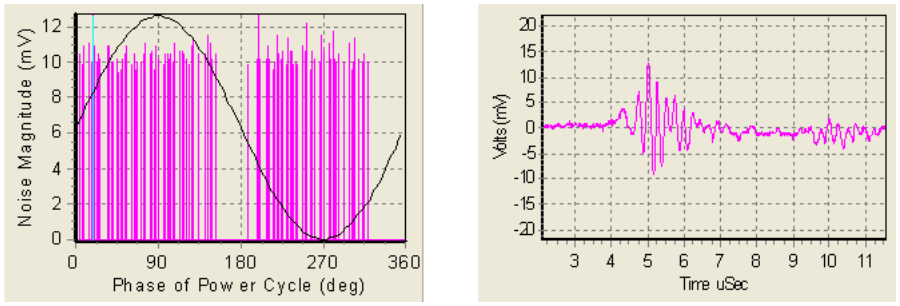

Figure 6.6: Noise Events and Segment Waveform of phase Y

Fig. 6.8 gives the noise signals and its segment waveform of phase B. Fig. 6.9 gives the switchgear PD and its segment waveform as captured by TEV probe.

Fig. 6.10 shows the number of PD pulses with respect to rise-time. For phase B,

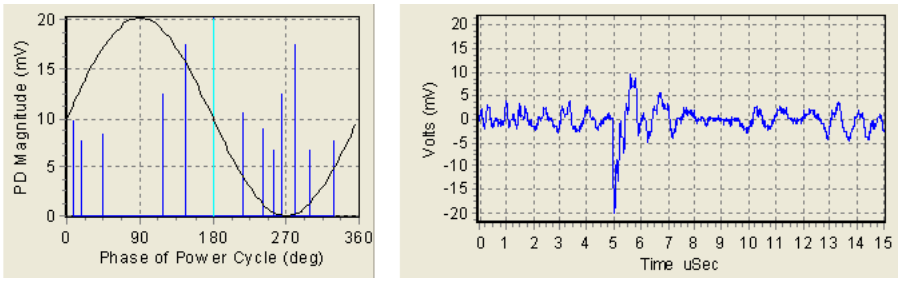

Figure 6.7: Machine PD of Phase B and Segment Waveform

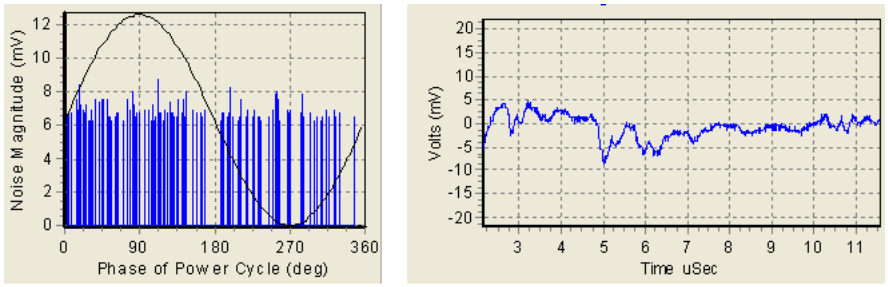

Figure 6.8: Noise Events of Phase B and Segment Waveform

the PD signals have rise-time in range of 15 ns to 110 ns. All the above results and observations from machine page show that PD in phase B is more comparative to other two phases. There is slot discharge i.e. phase/earth discharge in phase B, but the value is very less i.e. around 802 pC (<2000 pC). Show it can be said that the insulation of winding is in healthy condition and does not require any repair for replacement. It is wise to carry out PD measurement of the motor once in a year or while shut down and trend the consecutive results which can be used for future references.

6.3 On-line PD Testing ♯ 2

On-line partial discharge testing was done on three phase, 50Hz, 6.6kV HT motor. Here partial discharge within the insulation system of HV Motor is measured using three HFCT (High Frequency CT) sensors and one TEV (Transient Earth Voltage) probe. The HFCT sensors were clamped on the line side of each of the three phases of the motor and TEV probe was placed on the outer body of the terminal box. The

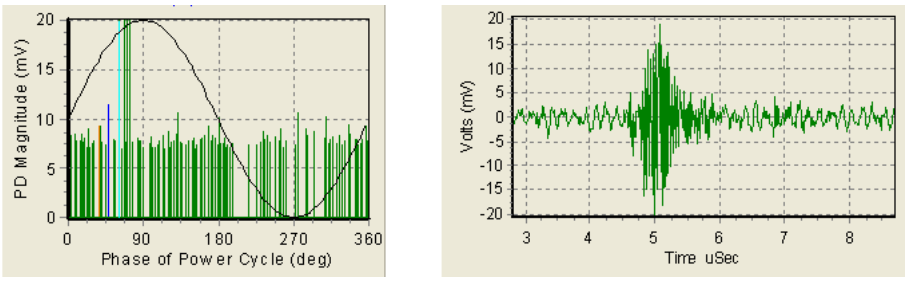

Figure 6.9: Switchgear PD as captured by TEV and highest segment Waveform

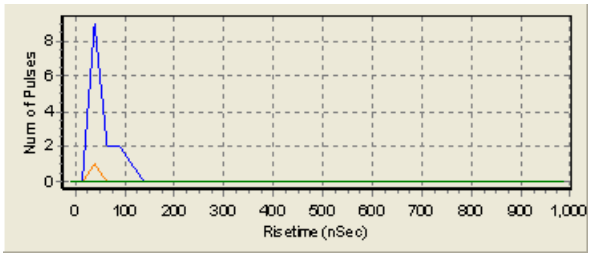

Figure 6.10: Number of pulses in Rise-time range

test set-up is as shown in the figure 6.11.

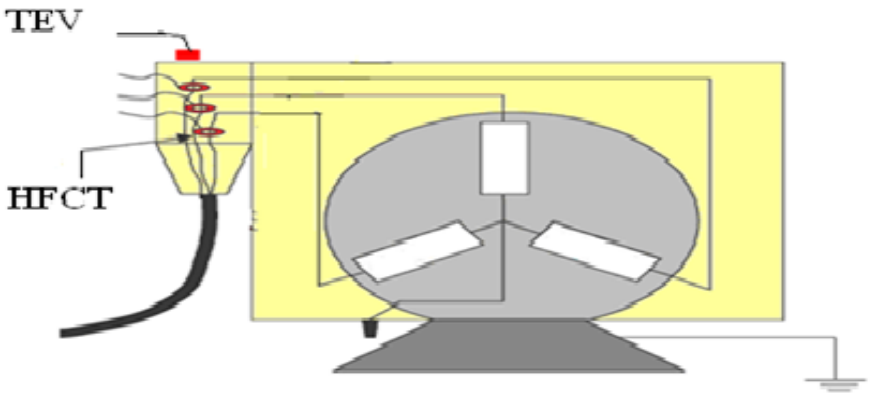

Figure 6.11: Test Set-up

The HFCT sensors are placed as close as possible to the line terminals to avoid major signal manipulation. Here all the three phases are tested online and simultaneously using HFCTs, i.e. motor is working at its operating voltage of 6.6kV and other working conditions. These sensors are connected to the DSO of PD measurement system on the other side. DSO has four channels. HFCT sensors clamped on R, Y

and B phase are connected to channel 1, 2 and 3 respectively. TEV probe is connected to channel 4. As part of the test it is important to ensure that the HV power supply and HV connections used in the test set-up are discharge-free.Table 6.3 shows the peak value of PD events in all the 4 channels, both in mV and pC.

Table 6.3: Peak PD Value of Different Phases

Sensor	*Phase*	*Peak PD Level in mV*	*Peak PD Level in pC*	*No. of PD Events*
HFCT	R	185.59	5660	124
HFCT	Y	18.56	407.6	21
HFCT	B	80.00	2490	52
TEV Probe	Frame	224.0	47dB	134

Figure 6.12 shows Peak PD magnitude of all the four channels with respect to time. Fig. 6.13 shows the PD data of all the channels across the power cycle.

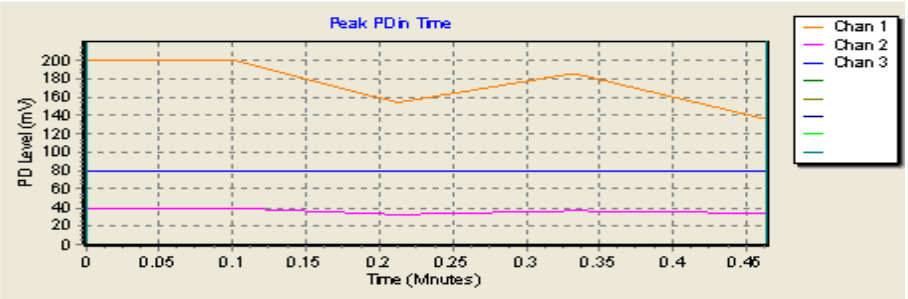

Figure 6.12: Peak amplitude v/s Time

The signals are captured at the sampling rate of 100MS/sec and 2M Samples are taken for each power cycle. For each acquisition 5 cycles are captured. The width of each PD segment waveform is 15sec. HFCT gives output in mV and depending upon its transfer impedance, the value of PD current in mA can be obtained. By integrating this current value, PD value in pC can be obtained. pC value depends upon rise time, fall time, amplitude of PD signal. If the signal travels more distance

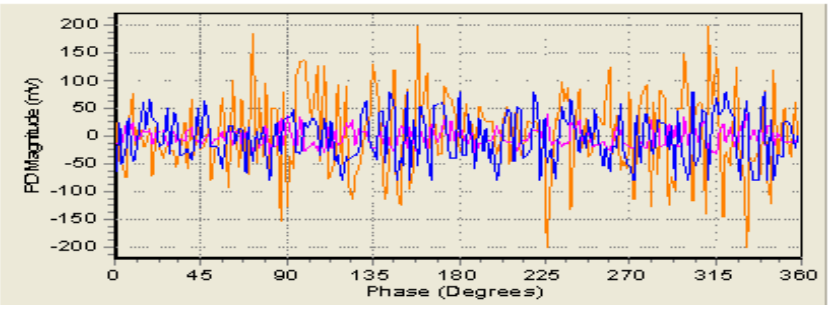

Figure 6.13: Cumulative PD data

between its origin and sensor location, then signal rise-time and fall time increases and amplitude decreases. This changes the value of signal pC as given by the sensor.

PD Activity in Phase R:

Fig. 6.14 shows the machine PD of phase R across power cycle and segment waveform of peak machine PD signal. Total 124 events of PD are recognized. All the other signals captured by sensor are either noise signals or switchgear PD signals. The peak PD value is 185.59 mV which corresponds to 5660pC depending upon its risetime, fall time and signal amplitude. Its rise time is 86.08 nSec and fall time is 90.02 nSec. Frequency of maximum amplitude is the frequency at which the signal peaks in the FFT frequency spectrum and its value is 1.12MHz.

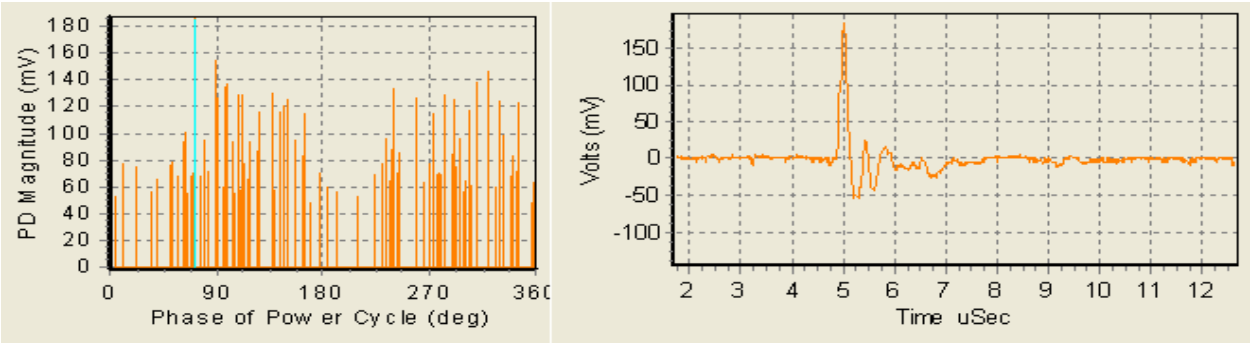

Figure 6.14: Machine PD and Highest Segment Waveform of Phase R

Fig. 6.15 shows the number of PD pulses with respect to rise-time. As shown in figure most of the signals have their rise time in the range of 30 nSec to 70 nSec. As per [11] the PD signals have their rise time in the range of few tens of nanoseconds. So the signals are in the required range of rise-time.

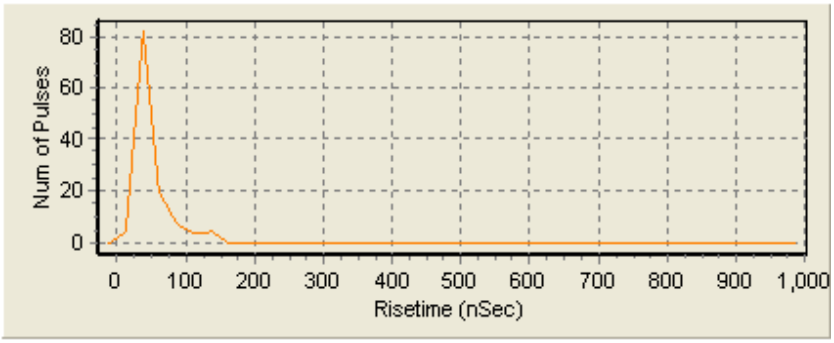

Figure 6.15: No. of Pulses in Rise-time Range

Fig. 6.16 shows the switchgear PD and segment waveform of highest signal of phase R. Its value is 89.6mV which corresponds to 39.05dB. Its frequency of maximum amplitude is 7.55MHz. Altogether 13 such events are recognized. Fig. 6.17 shows the noise signals and segment waveform of highest noise signal. Its amplitude is 56mV, rise time is 143.24 nSec and fall time is 102.6 nSec. Frequency of maximum amplitude is 752 kHz.

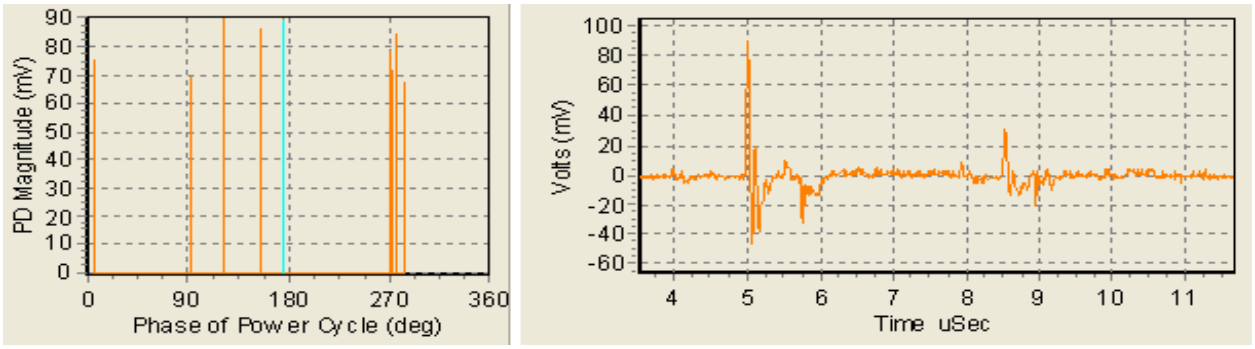

Figure 6.16: Switchgear PD and Segment waveform of Phase R

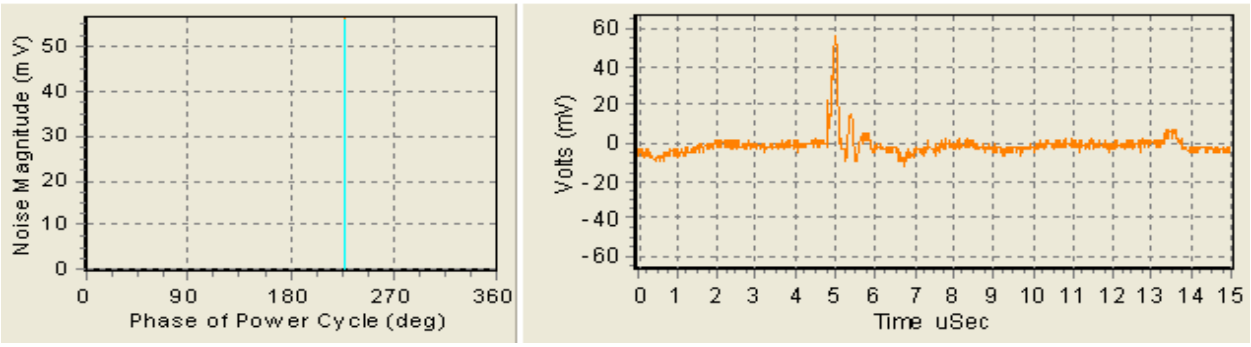

Figure 6.17: Noise Event of Phase R and its Segment Waveform

PD Activity in Phase Y:

Fig. 6.18 shows the machine PD of phase Y across power cycle and segment waveform of peak machine PD signal. Total 21 events of PD are recognized. All the other signals captured by sensor are either noise signals or switchgear PD signals. The peak PD value is 18.56 mV which corresponds to 407.6 pC depending upon its risetime, fall time and signal amplitude. Its rise time is 61.44 nSec and fall time is 79.77 nSec. Frequency of maximum amplitude is the frequency at which the signal peaks in the FFT frequency spectrum and its value is 1.23MHz.

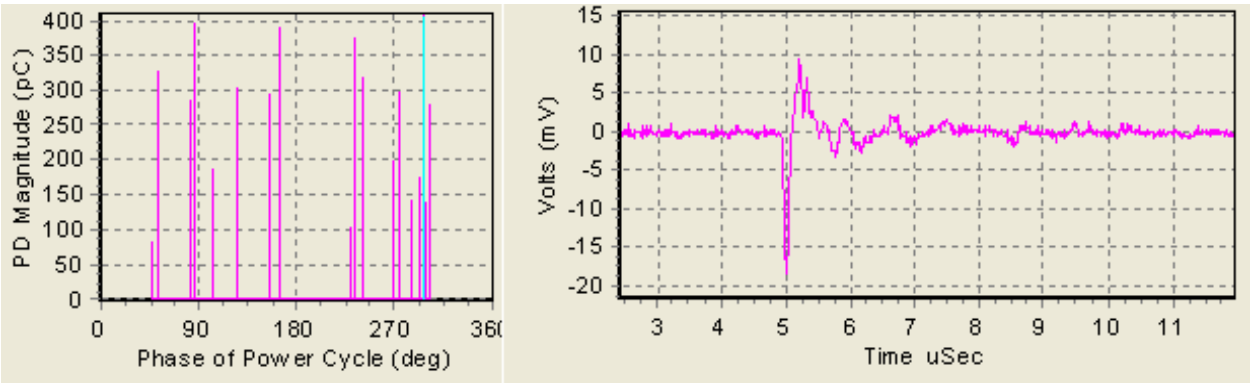

Figure 6.18: Machine PD and Highest Segment Waveform of Phase Y

Fig. 6.19 shows the number of PD pulses with respect to rise-time. As shown in figure most of the signals have their rise time in the range of 18 nSec to 85 nSec. As

per [11], the signals are in the required range of rise-time.

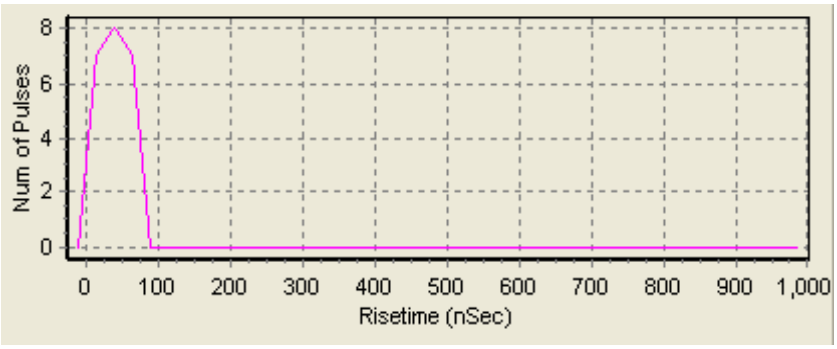

Figure 6.19: No. of Pulses in Rise-time Range

Fig. 6.20 shows the switchgear PD and segment waveform of highest signal of phase Y. Its value is 40.0 mV which corresponds to 32.04dB. Its frequency of maximum amplitude is 8.22MHz. Altogether 80 such events are recognized. Fig. 6.21 shows the noise signals and segment waveform of highest noise signal.

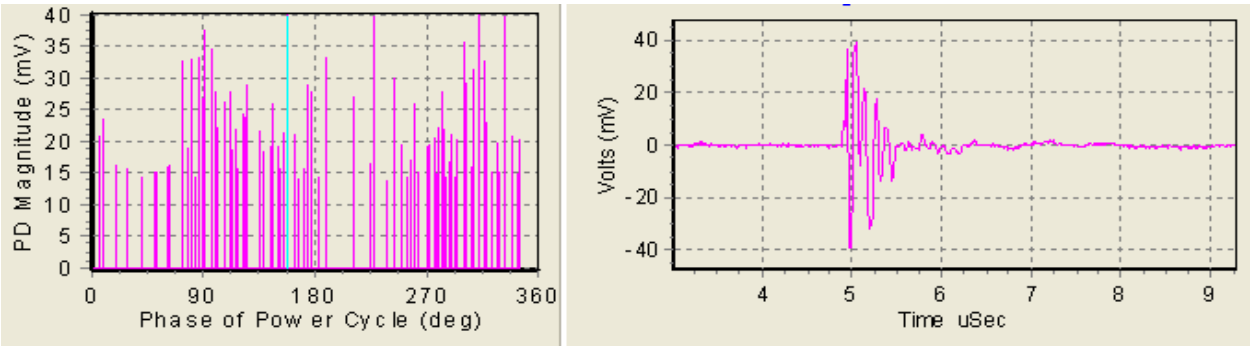

Figure 6.20: Switchgear PD and Segment waveform of Phase Y

PD Activity in Phase B:

Fig. 6.22 shows the machine PD of phase B across power cycle and segment waveform of peak machine PD signal. Total 52 events of PD are recognized. All the other signals captured by sensor are either noise signals or switchgear PD signals. The peak PD

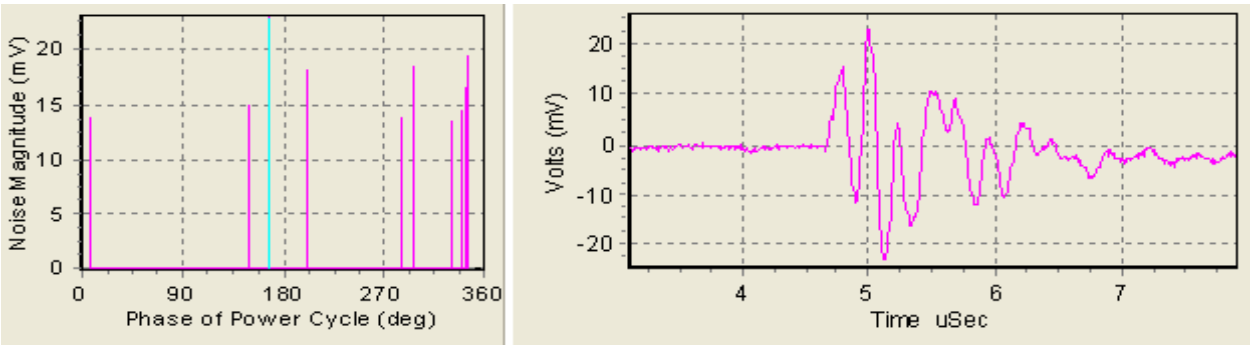

Figure 6.21: Noise Event of Phase Y and its Segment Waveform

value is 80.0 mV which corresponds to 2490 pC depending upon its rise time, fall time and signal amplitude. Its rise time is 90.02 nSec and fall time is 86.32 nSec. Frequency of maximum amplitude is the frequency at which the signal peaks in the FFT frequency spectrum and its value is 2.13MHz.

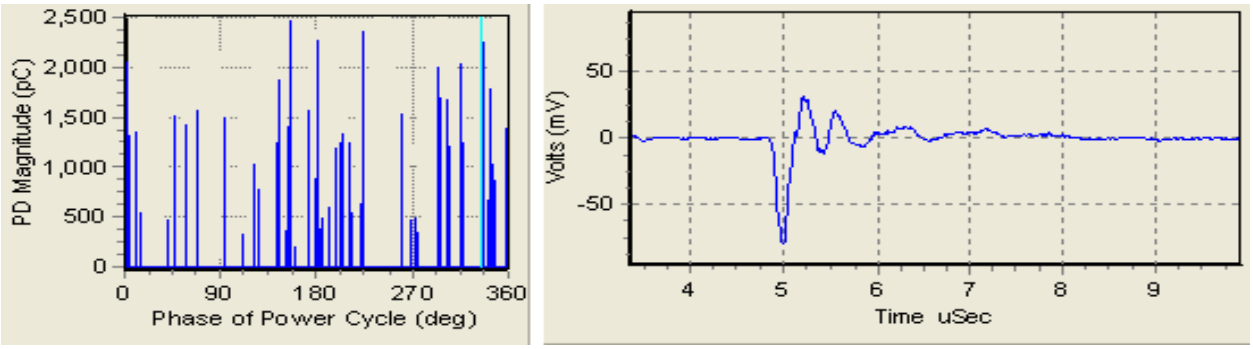

Figure 6.22: Machine PD and Highest Segment Waveform of Phase B

Fig. 6.23 shows the number of PD pulses with respect to rise-time. As shown in figure most of the signals have their rise time in the range of 18 nSec to 95 nSec. As per [11], the signals are in the required range of rise-time. Fig. 6.24 shows the switchgear PD and segment waveform of highest signal of phase B. Its value is 51.84 mV which corresponds to 34.29dB. Its frequency of maximum amplitude is 31.82MHz. Altogether 21 such events are recognized.

Fig. 6.25 shows the noise signals and segment waveform of highest noise signal. Its

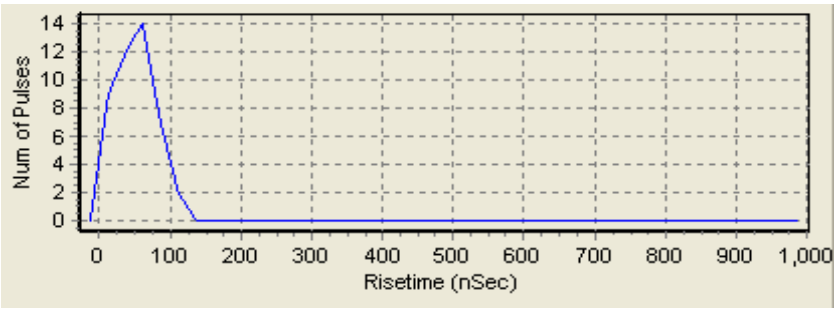

Figure 6.23: Number of pulses in Rise-time range

peak magnitude is 48mV. Rise time is 120 nSec and fall time is 83 nSec. Total 8 noise signals are recognized. Fig. 6.26 shows the switchgear PD signals as captured by TEV sensor. Also segment waveform of highest signal is shown. Total 134 switchgear signals are recognized. Its peak value is 224mV which corresponds to 47dB. Its frequency of maximum amplitude is 9.09MHz. Rise time and fall time of signal are 12.21 nSec and 13.41 nSec respectively.

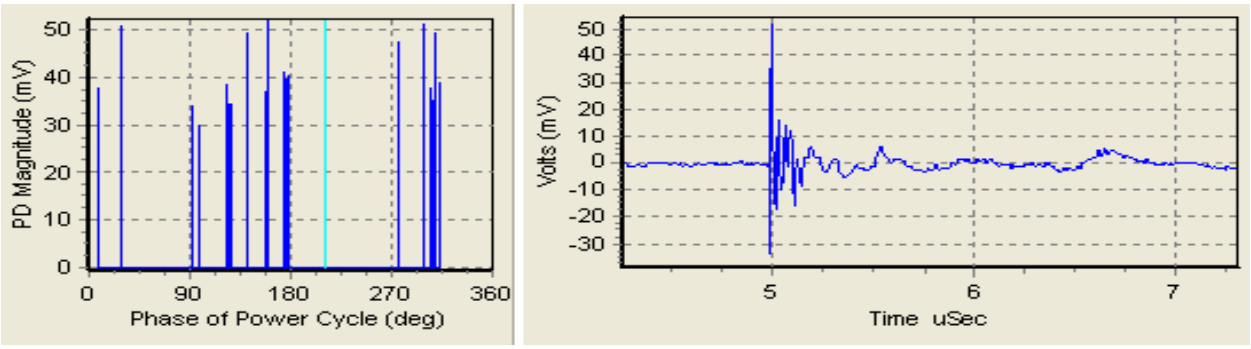

Figure 6.24: Switchgear PD and Segment waveform of Phase B

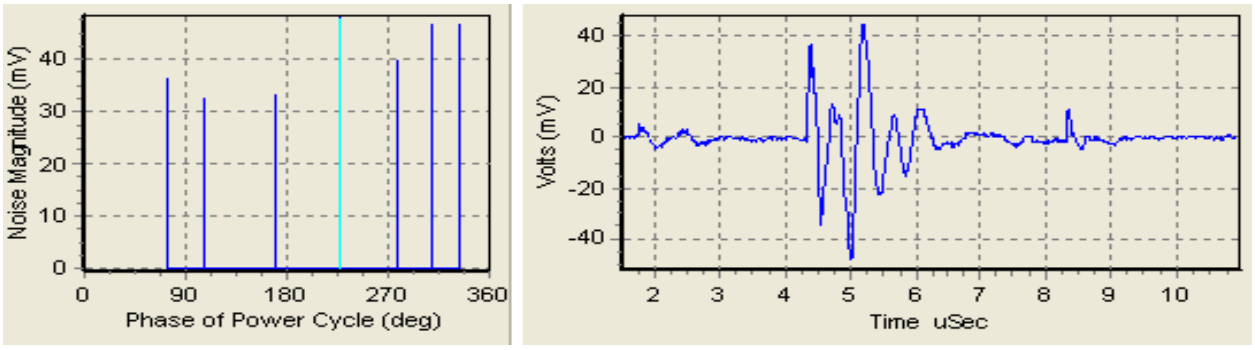

Figure 6.25: Noise Event of Phase B and its Segment Waveform

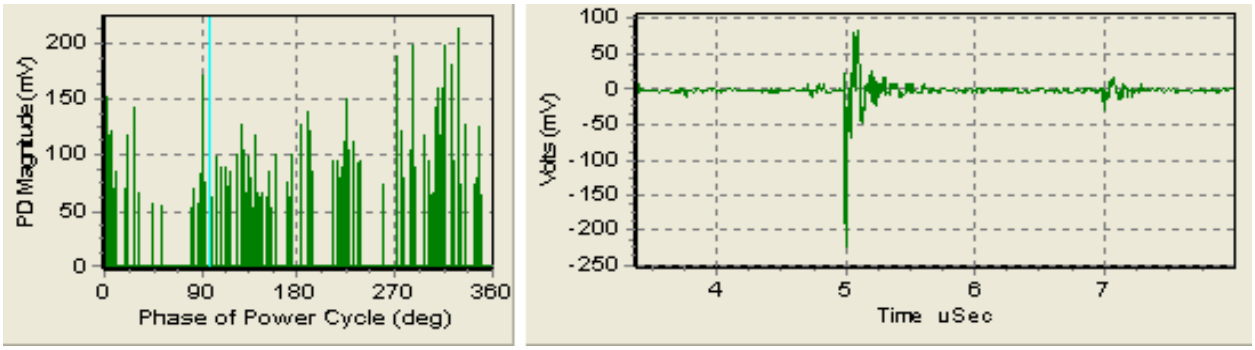

Figure 6.26: Switchgear PD and its Segment waveform From TEV Sensor

6.3.1 Inferences

Phase R

In phase R total 124 PD events have been recognized. The peak PD value is 5660pC. Fig. 6.27 shows the highest segment waveform of machine PD signal of phase R. Its is measured synchronously with phase Y and Phase B. As shown in figure when PD event occurs in phase R at that time there is no PD event of phase Y and phase B which is in-phase with phase R. So it can be said that there is a slot discharge in phase R. So it can be said that insulation condition of phase R is average and there is slot discharge in phase R. Number of positive and negative PD events are almost equal, so it can be said that discharge source may be within the insulation of winding.

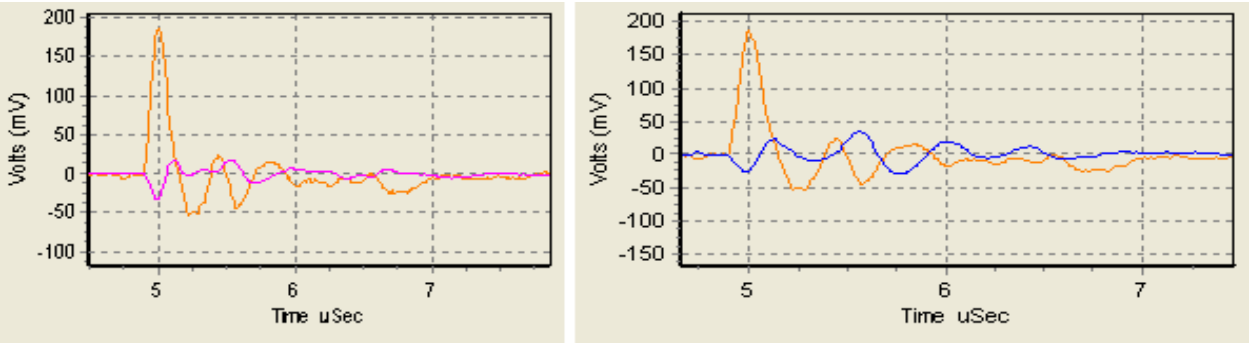

Figure 6.27: Segment Waveform of Phase R Synchronously measured with phase Y and B

Phase Y

In phase Y total 21 PD events have been recognized. The peak PD value is 407 pC. When PD event occurs in phase Y at that time there is no PD event of phase R and phase B which is in-phase with phase Y. So it can be said that there is a slot discharge in phase Y. But as number of PD events are very less and also peak PD value is very less, so it can be said that insulation condition of phase Y is excellent.

Phase B

In phase B total 52 PD events have been recognized. The peak PD value is 2490pC. For phase B also when PD event occurs in phase B at that time there is no PD event of phase Y and phase R which is in-phase with phase B. So it can be said that there is a slot discharge in phase B. As the number of PD events are more and peak PD magnitude is also more it cannot be said that the insulation condition is excellent. But as the magnitude is not very high so it can be said that insulation condition of phase B is good and there is slot discharge in phase B. Number of positive and negative PD events are almost equal, so it can be said that discharge source may be within the insulation of winding. So it can be inferred that at present motor insulation condition

is good for phase Y and B and average for phase R. For machines with 6kV or more voltage rating, it is wise to carry out PD measurement of the machine once in every 6 months. For 4kV voltage rating machines, testing should be done more frequently as there is short-time frame between detection and failure for these motors.

6.4 Off-line PD Testing

Partial discharge within the insulation system of 3-phase, 50 Hz, 11kV, 56.3MW, HT turbo generator is measured using Coupling Capacitor as sensor. The Coupling Capacitor (850 pC, 24kV) is connected in parallel with the machine under test as shown in fig. 6.28. Voltage is fed to each individual winding (phase) one at a time and the other remaining windings are grounded while measurement. Voltage is increased in steps to find the PD inception voltage of that particular phase. PD value in pC can be obtained using calibration constant. Similarly other two phases are also measured.

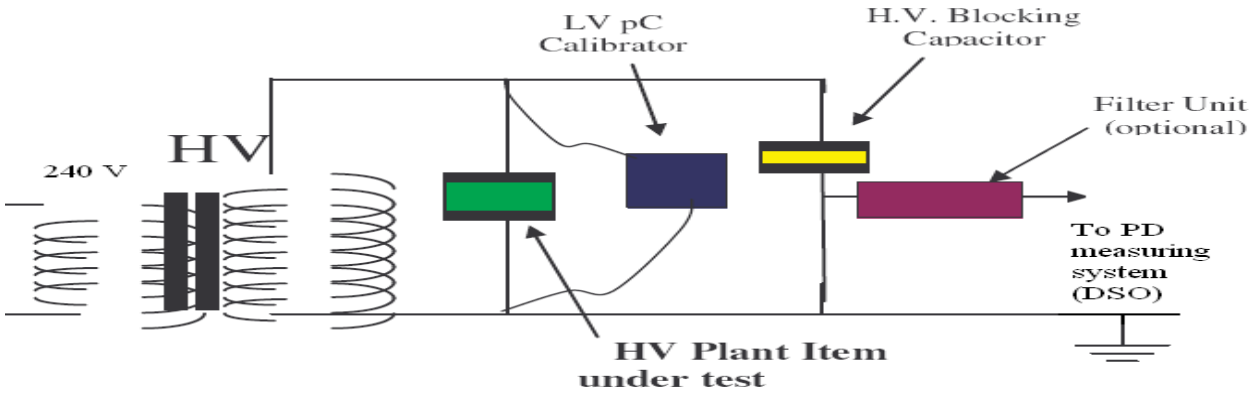

Figure 6.28: Test Set-up

The lower cut-off frequency of 850pF coupling capacitor is 185 KHz. Coupling capacitor has to be calibrated by using a low voltage calibrator at testing site. So calibration constant in pC/mV can be obtained for PD measurement in pC.Here LV pC calibrator is used having value 8000pF. A known value of charge is injected in

test sample using a voltage generator giving 1V and calibrator. Thus total 8000pC is injected and output in mV is obtained. Thus calibration constant is obtained in pC/mV. The pc calibrator is then removed from test circuit and tests are carried out. It is normal practice to test each phase of the machine in turn with a single-phase Blocking Capacitor to fully quantify and locate PD activity on a phase-by-phase basis. As part of the test it is important to ensure that the HV power supply and HV connections used in the test set-up are discharge-free. The output from coupling capacitor is given to channel 1 of DSO. Measured PD level of each individual phases at different test voltage are given below in table 6.4.

Table 6.4: PD Values at Different Voltages

Phase	*Applied Voltage in kV*	*Peak PD Level in pC*	*Peak PD Level in mV*
R	4	731.4	57.6
R	6	838.06	390.38
Y	4	1020	38.40
Y	6	2580	371.19
B	4	1280	44.80
B	6	2210	204.79

6.4.1 PD Activity in Phase R

At 4kV

PD activity is present at 4kV. Fig. 6.29 shows the machine PD and the Segment waveform of highest Machine PD event. The calibration constant for R phase is 12.13 pC/mV. Peak PD value is 57.60 mV which corresponds to 699 pC but depending upon risetime, fall time and amplitude it gives 731.40pC value. Its rise time is 23.02 nSec and fall time is 64.45 nSec which satisfy the range of PD signals as given by [11]. Frequency of maximum amplitude is the frequency at which the signal peaks in the FFT frequency spectrum and its value is 1.79MHz. Only two PD events are recognized. Fig. 6.30 shows switchgear PD and noise events at 4kV.

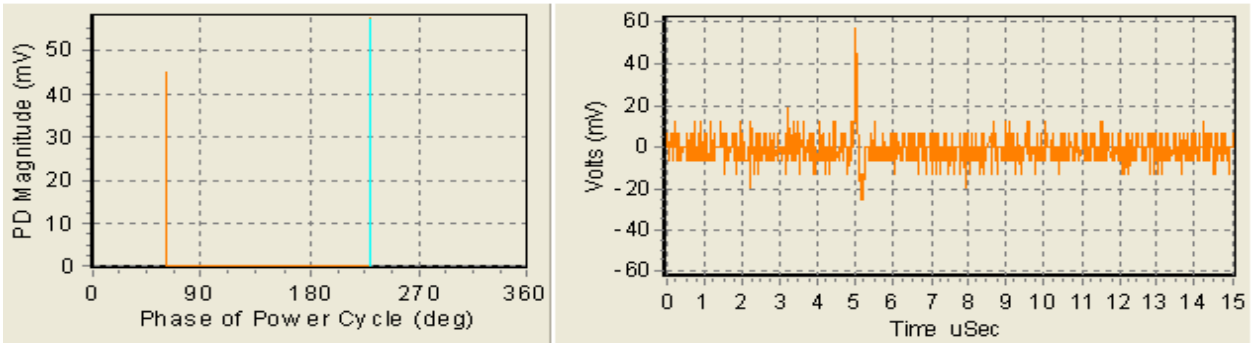

Figure 6.29: Machine PD and Segment Waveform of Highest Machine PD at 4kV

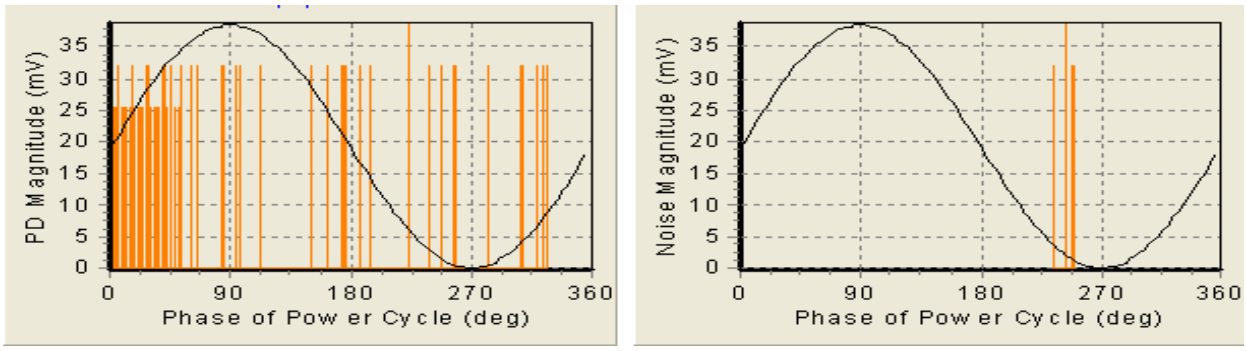

Figure 6.30: Switchgear PD and Noise events at 4kV

At 6kV

At 6kV initially no PD signals were identified as the switchgear PD signals lower limit is set to 4.5MHz. Then from switchgear PD events nine machine PD events are identified based upon pD signal characteristics i.e. rise time, fall time, pulse shape. Fig. 6.31 shows the machine PD and the Segment waveform of highest Machine PD event. Its value is 390.38mV which corresponds to 4737pC but depending upon risetime, fall time and amplitude it gives only 838.38pC value. Its rise time is 13.81 nSec and fall time is 12.45 nSec. Frequency of maximum amplitude is 25MHz. Fig. 6.32 shows switchgear PD and noise events at 4kV.

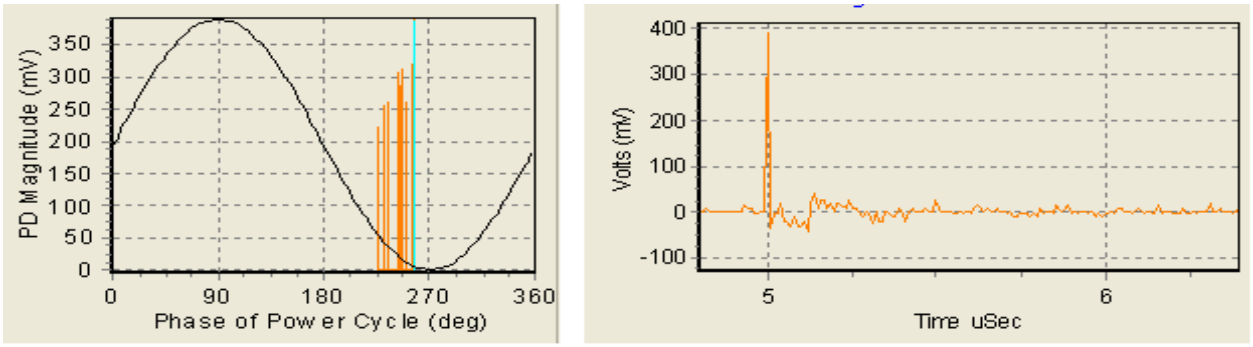

Figure 6.31: Machine PD and Segment waveform of Highest signal at 6kV

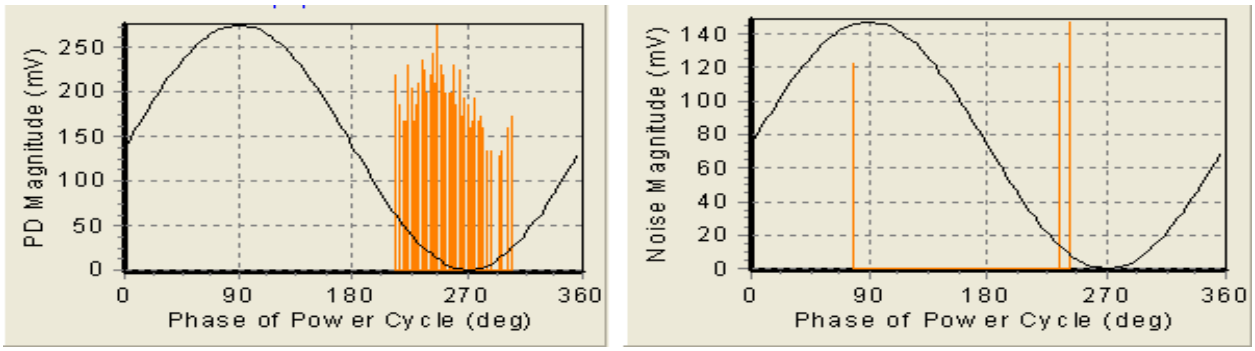

Figure 6.32: Switchgear PD and Noise events at 6kV

6.4.2 PD Activity in Phase Y

At 4kV

Nine PD events are identified at 4kV. Calibration constant of phase Y is 13.157 pc/mV. Fig. 6.33 shows the machine PD and the Segment waveform of highest Machine PD event. Its value is 38.40mV which corresponds to 505.2pC but depending upon risetime, fall time and amplitude it gives 1020pC value. Its rise time is 52.94 nSec and fall time is 115.10 nSec. Frequency of maximum amplitude is 1.20MHz. Here the negative PD events are more in number compared to positive PD events.

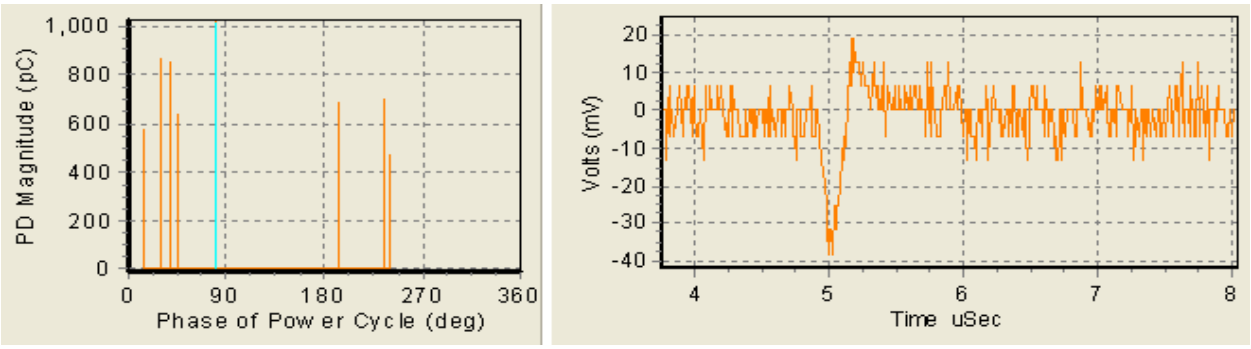

Figure 6.33: Machine PD and Segment Waveform of phase Y at 4kV

At 6kV

Considerable PD events are identified at 6kV. Fig. 6.34 shows the machine PD and the Segment waveform of highest Machine PD event. Its value is 371.19mV which corresponds to 4883pC but depending upon risetime, fall time and amplitude it gives 2580pC value. Its rise time is 17.38 nSec and fall time is 36.67 nSec. Frequency of maximum amplitude is 2.13MHz. Here the positive PD events are more in number compared to negative PD events.

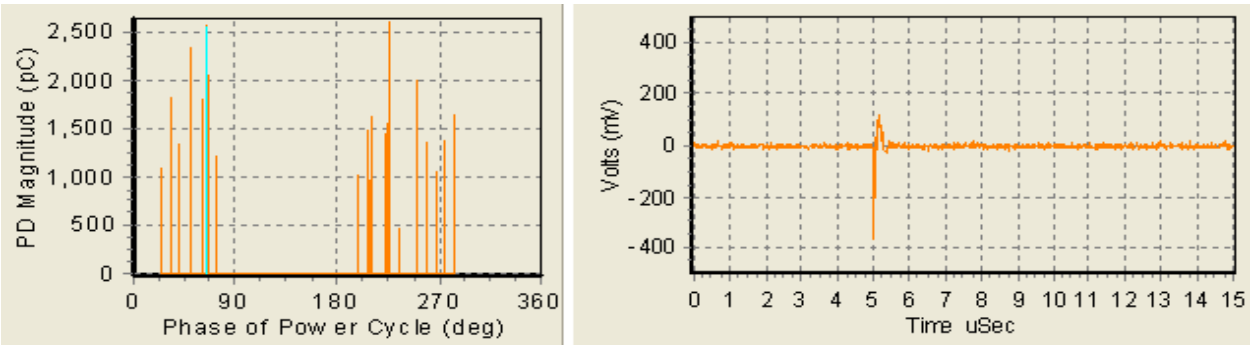

Figure 6.34: Machine PD and Segment waveform of phase Y at 6kV

Fig. 6.35 shows the number of pulses in rise-time range. As shown in figure, all the pulses have their risetimes in the range of 15 to 25 nSec. The signals have their rise time in the range of few tens of nanoseconds [11]. As signal travels from its place of

origin to the sensor, the signal gets deteriorated and hence its shape changes. So its amplitude decreases and frequency also decreases. So pC value obtained increases. Hence sensors should be placed as close as possible to the winding.

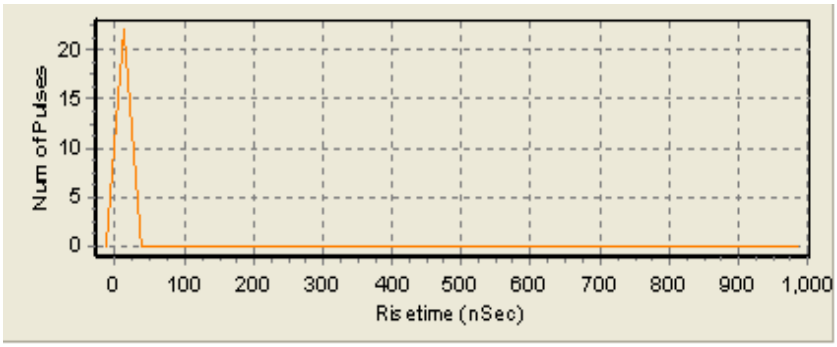

Figure 6.35: No. of Pulses in Risetime Range

6.4.3 PD Activity in Phase B

At 4kV

Seven PD events are identified at 4kV. Calibration constant of phase B is 12.37 pC/mv. Fig. 6.36 shows the machine PD and the Segment waveform of highest Machine PD event. Its value is 44.8 mV which corresponds to 554.17pC but depending upon risetime, fall time and amplitude it gives 1280pC value. Its rise time is 57.22 nSec and fall time is 122.33 nSec. Frequency of maximum amplitude is 2.78MHz. Here also the rise time of pulses is in the range of 25-60 nSec. Here the negative PD events are more in number compared to positive PD events.

At 6kV

Eight PD events are identified at 6kV. Fig. 6.37 shows the machine PD and the Segment waveform of highest Machine PD event. Its value is 204.79 mV which corresponds to 2533pC but depending upon rise-time, fall time and amplitude it gives 2210pC value. Its rise time is 18.13nSec and fall time is 58.27nSec. Frequency of

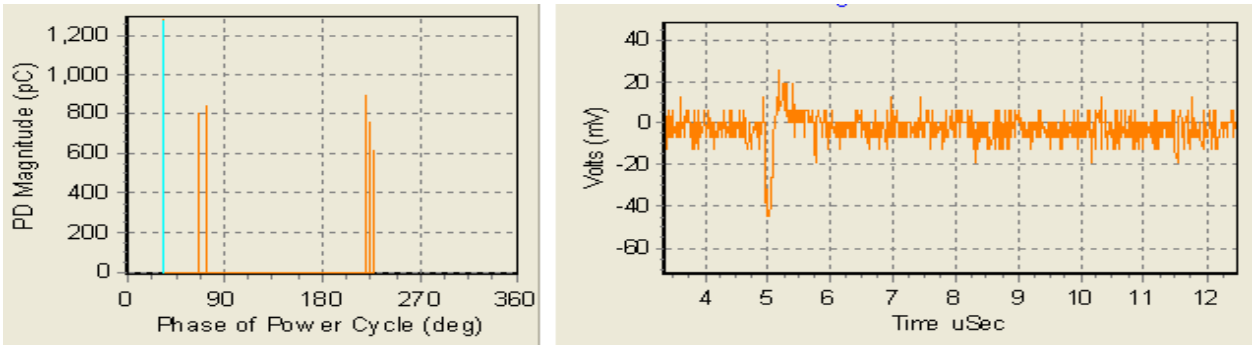

Figure 6.36: Machine PD and Segment waveform of phase B at 4kV

maximum amplitude is 2.0MHz. Here also the rise time of pulses is in the range of 15-25 nSec. Fig. 6.38 shows the PRPD pattern of phase B. It resembles to the PRPD pattern of slot discharges. Here the positive PD events are more in number compared to negative PD events. Fig. 6.39 shows the ideal Slot discharge PRPD pattern as per [18].

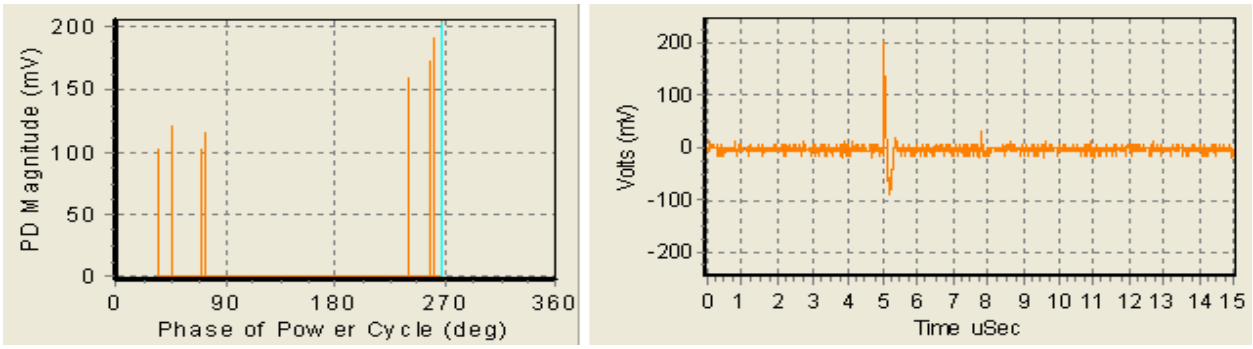

Figure 6.37: Machine PD and Segment waveform of phase B at 6kV

6.4.4 Inferences

Phase R: In Phase R, PD activity is present at both 4kV and 6kV. The amplitude increases from 57mV to 390mV as voltage is increased. It corresponds to around 838pC value. Also number of PD events is not very high. So it can be said that

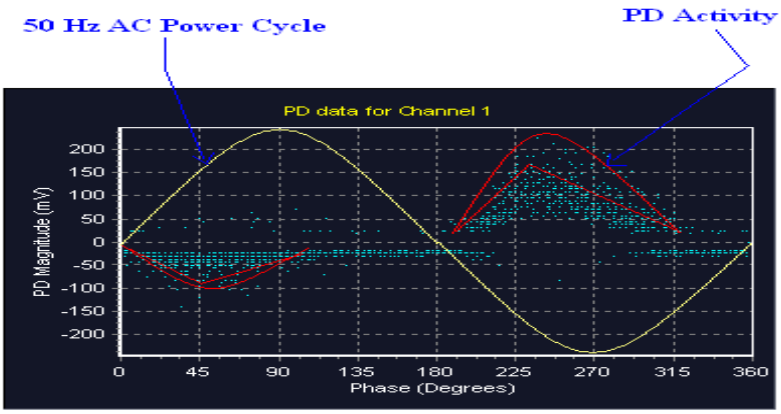

Figure 6.38: PRPD Pattern of Phase B at 6kV

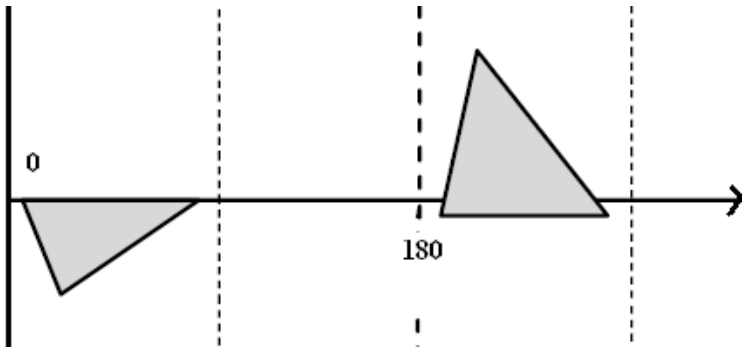

Figure 6.39: Ideal Slot Discharge PRPD Pattern

insulation condition of phase R is in excellent condition.

Phase Y: In phase Y, PD activity is present. Its amplitude increases from 38.4mV to 371mV, which corresponds to 1020pC to 2580 pC as voltage level increases. Also number of PD events increases considerable. So it can be said that insulation condition of phase Y is not excellent but since the PD events are not very high and pC value is also less, it can be said that winding condition is good. But as positive PD events are more so it can be said that there may be PD source in slot portion. Also discharge source may be present between the main insulation and the copper conductor [19].

Phase B: In phase B also PD events are recognized. The magnitude of PD pulses

increases from 44.8mV to 204.8mV as voltage increases. The PD value in pC increases from 1280 to 2210pC. The PD magnitude is more but no. of PD events are less. So it can be said that insulation condition of the winding is in good condition. Its PRPD pattern resembles to slot discharges. Slot discharges are characterized by negative PD pulses occurring at 45degress and positive pulses occurring at 225degrees of 50 Hz AC power cycle. Slot discharges are also characterized by asymmetry with larger positive discharges during the negative portion of the cycle, asymmetry in the amount of discharge, sharp declining gradient during the negative half cycle giving a triangular shape. So it can be said that it is slot discharge. Also as positive PD events are more as compared to negative PD events. so it can be said that PD source is in the space between insulation surface and iron core. Also at 4kV, negative PD is more, so it can be said that their may be PD source at interface between conductor surface and insulation.

So it can be inferred that generator stator insulation condition is good at present. For machines with 6kV or more voltage rating, it is wise to carry out PD measurement of the machine once in every 6 months. For 4kV voltage rating machines, testing should be done more frequently as there is short-time frame between detection and failure for these motors

6.5 Validation of Experimental Results

Using wavelet transformation technique for denoising, PD signals can be separated from noise signals depending upon pulse shape. This separation depends upon mother wavelet selection, threshold level and number of decomposition level.

Here the experimental results that are carried out using PD test system are verified with theoretical conclusions. The machine PD of phase B of motor as given in on-line PD testing 1 and segment waveform of highest PD event is shown in fig. 6.40. Its rise-time is 54.31 nSec. Frequency of maximum amplitude is 1.2 MHz. So its

characteristics metches with PD signals. Also its shape matches with mother wavelet. Thus it is recognized as machine PD signal. Fig. 6.41 shows noise signals. Its shape does not match with that of pD also its rise time is high. Thus it is separated as noise signal. Thus noise separation is done accordingly for all signals.

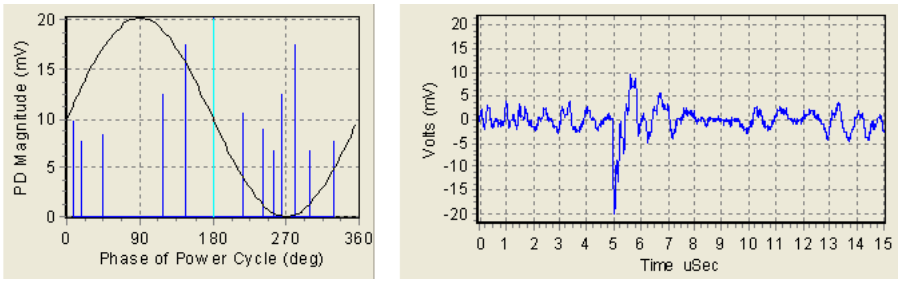

Figure 6.40: Machine PD of Phase B and Segment Waveform

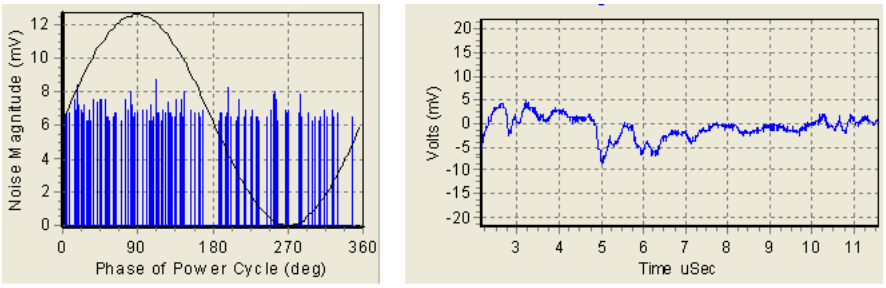

Figure 6.41: Noise Events of Phase B and Segment Waveform

Fig. 6.42 shows the segment waveform of PD signal coming from R phase of 6.6 kV motor as given in on-line PD testing 2, measured by HFCT. These signals are captured with db4 selected as mother wavelet. As seen from Fig. 5.9 and Fig. 6.42, the shape of segment waveform of PD signal matches with that of wavelet waveform shape. PD signals have their rise-time in the range of few nano-seconds [11]. Also the signals have their frequency spectrum in the range of few MHz. The PD signal segment which is captured has characteristics that matches with that of PD signal. Its frequency of maximum amplitude is 1.12MHz, rise-time is 80.2 nSec. So using wavelet transformation technique PD signals are separated from noise signals and total 124 such events are separated as PD signals.

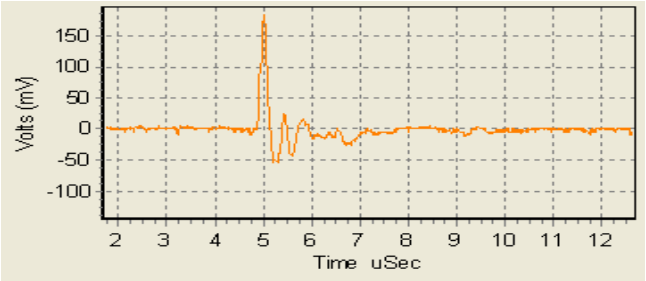

Figure 6.42: Segment Waveform of PD signal of phase R

Fig. 6.43 shows machine PD signal of phase Y. Total 21 events of PD are recognized. Its rise time is 61.44 nSec and fall time is 79.77 nSec. Frequency of maximum amplitude is the frequency at which the signal peaks in the FFT frequency spectrum and its value is 1.23MHz. Thus the segment waveform matchs with P signal.

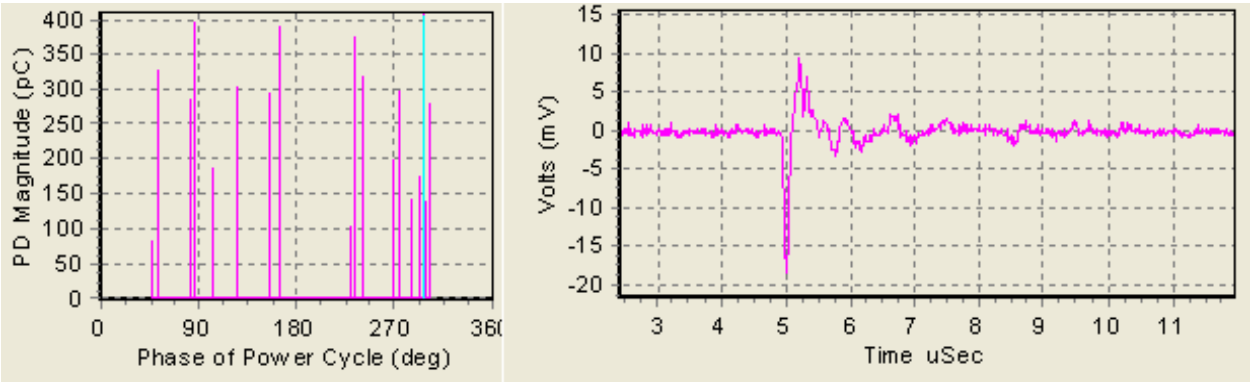

Figure 6.43: Machine PD and Highest Segment Waveform of Phase Y

Similarly, Fig. 6.44 shows machine PD signal of phase B. Its rise time is 90.02 nSec and fall time is 86.32 nSec. Frequency of maximum amplitude is 2.13MHz.

Similarly segment waveforms of PD signals of Phase R, Y and B at 6kV of motor, which is given in off-line PD testing results, are shown in Fig. 6.45, fig. 6.46 and

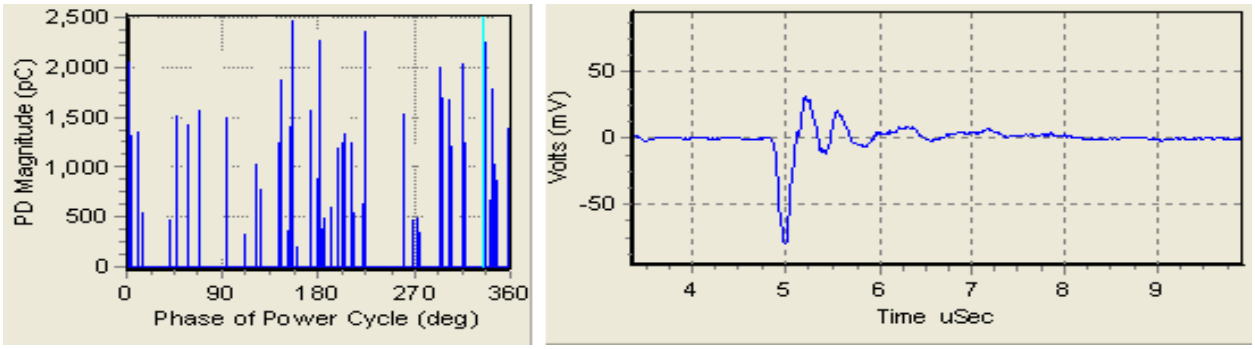

Figure 6.44: Machine PD and Highest Segment Waveform of Phase B

fig. 6.47 respectively. Phase R has signal with rise time 13.81 nSec and fall time 12.45 nSec. Frequency of maximum amplitude is 25MHz. Phase Y has rise time equal to 17.38 nSec and fall time of 36.67 nSec. Frequency of maximum amplitude is 2.13MHz. Phase B has rise time of 18.13nSec and fall time of 58.27nSec. Frequency of maximum amplitude is 2.0MHz. All these signals have PD like characteristics and also their shape matches with mother wavelet shape. Thus PD signals are separated from noise signals.

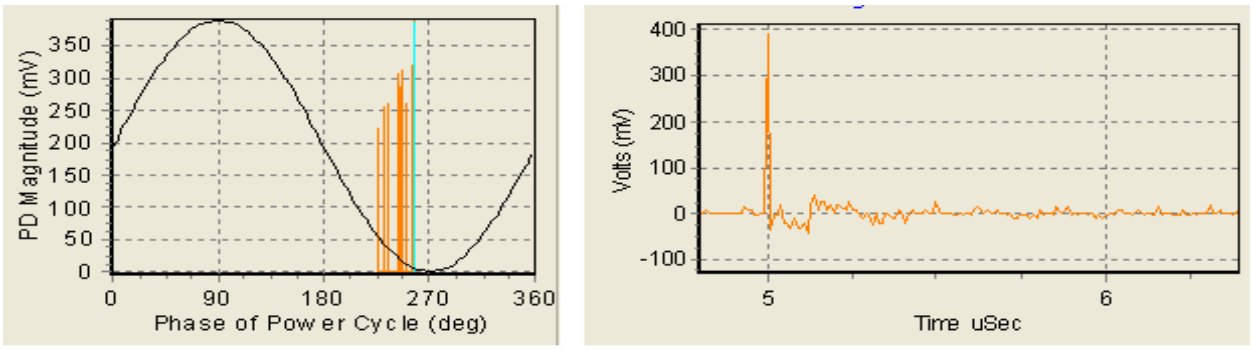

Figure 6.45: Machine PD and Segment waveform of Highest signal at 6kV of R

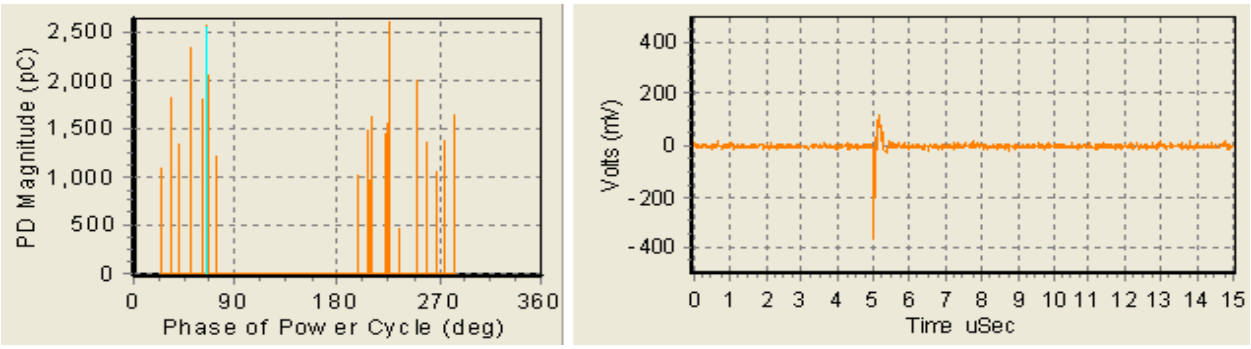

Figure 6.46: Machine PD and Segment waveform of phase Y at 6kV

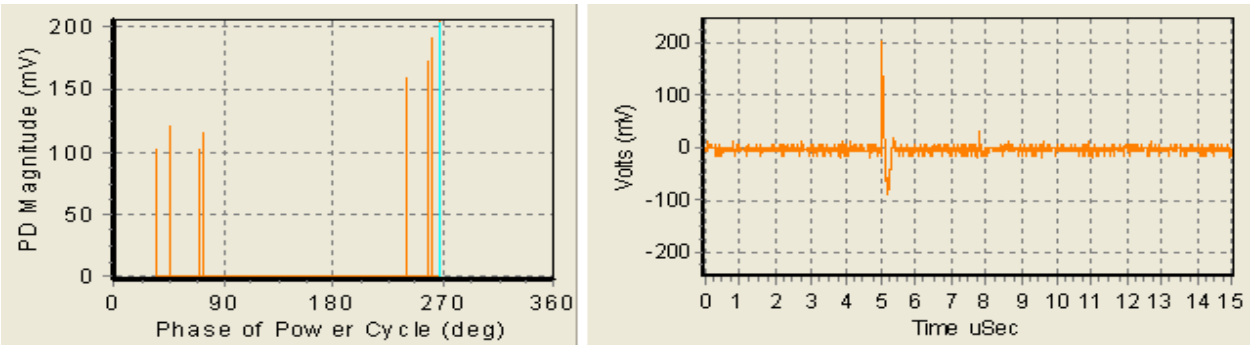

Figure 6.47: Machine PD and Segment waveform of phase B at 6kV

Chapter 7

Conclusion and Future Scope

7.1 Conclusion

Data obtained through Partial Discharge Testing and Monitoring can provide critical information on the quality of insulation and its impact on overall equipment health. Because PD activity is often present well in advance of insulation failure, asset managers can monitor it over time and make informed strategic decisions regarding the repair or replacement of the equipment. These predictive diagnostics help companies to prioritize capital before an unexpected outage occurs. Thus partial discharge testing is must for high voltage equipments.

Online PD testing is advantageous as it provides continuous monitoring at real operating conditions and it is economical than offline method. So on-line PD testing is preferred over offline PD testing.

PD testing was done on HV equipments using laboratory set-up and PD test system. As results matched, so it can be concluded that On-line PD testing is very much applicable to HV rotating electrical machines. On-line and off-line PD testing was done On-site on HV rotating machines using sensors such as HFCT, coupling capacitor, TEV probe and PD measurement system. The results show PD activity in some phases of machines and the value of PD in pC is known. This gives the indication

of the stator winding insulation condition. So PD measurement on rotating machines gives early indication of developing faults and thus it allows maintenance personnel to plan for repair and replacement.

On-line PD testing was done using CC, HFCT and TEV sensors. Coupling capacitor has better sensitivity as compared to other sensors, but it can be used for on-line testing only if it is already permanently installed with the machine. Ferrite core, HFCT is widely used as it can be easily connected due to its split-core type of construction.

The analysis of the on-line PD measurement results is difficult because of presence of wide variety of noise on-site. Thus noise signals should be separated from PD signals. Out of various methods, Wavelet Transformation (WT) technique provides better noise rejection in any harsh conditions. Signals are captured at very high acquisition rate and thus provide the information about the characteristics of PD signals such as rise-time, falltime, pulse width. Using WT technique and PD pulse shape analysis, the cause for PD generation and its location can be detected. Successful categorization or identification of different pulse shapes will enable diagnosis and localization of defect site and lead to better diagnosis results.

7.2 Future Scope

In On-line PD measurement, noise is a major problem. Many times noise signals mask the original PD signals and thus analysis of signals become difficult. So selection of noise separation technique is a major issue. Various noise rejection techniques are available, out of which wavelet transformation is robust one. Denoising is based upon mother wavelet selection and thresholding. So experiments can be done with different families of wavelet and thresholding level to properly separate noise from PD signals. Also experiments can be done with automated wavelet selection technique where optimal mother wavelet is selected automatically.

References

[1] M S Naidu and V Kamaraju, "High Voltage Engineering" 3rd edition, Tata Mc Graw-Hill, New Delhi, 2006, pp. 93-97 & pp. 379-387

[2] A.J.M. Pemen, P.C.T. van der Laan and W. De Leeuw, "Analysis and localization of spurious partial discharge activity in generator units" in proc. 2001 IEEE 7th International Conference on Solid Dielectrics, pp. 489-492

[3] Wijnand R. Rutgers, Robert Ross & Theo G.M. van Rijn, "On-line PD detection techniques for assessment of the dielectric condition of HV components" in proc. 2001 IEEE 7th International Conference on Solid Dielectrics, pp. 481-484

[4] Yafei Zhou, MIEEE, A I Gardiner, G A Mathieson, Y Qin, "New methods of partial discharge measurement for the assessment and monitoring of insulation in large machines", in proc. 1997 Electrical Insulation Conference and Electrical Manufacturing & Coil Winding Conference, pp. 111-114

[5] G. C. Stone, V. Warren, "Advancements in interpreting Partial Discharge test results to assess stator winding condition", Iris Power Enginnering

[6] IEC 60270 (2000): High-voltage test techniques - Partial discharge measurements

[7] R. Bartnikas and J. P. Novak, "Effect of overvoltage on the rise time and amplitude of partial discharge pulses", IEEE Transactions on Dielectrics and Electrical Insulation, Vol. 2, (4):557-566, 1995.

[8] Hutter, W., "Partial discharge detection in rotating machines", IEEE Electrical Insulation Magazine, Vol. 8, No. 3, pp. 21-32, May/June 1992

[9] Wilson, A., "Slot discharge damage in air cooled stator windings", Proceedings of the Institution of Electrical Engineers, Vol. 138A, No. 3, pp. 153-160, May 1991

[10] Emery, F. T., and Harrold, R. T., "On line incipient arc detection in large turbine generator stator windings", IEEE Transactions on Power Apparatus & Systems, Vol. PAS-99, No. 6, pp. 2232-2240, Nov./Dec. 1980.

[11] IEEE 1434 (2000): IEEE Trial-Use Guide to the Measurement of Partial Discharges in Rotating Machinery

[12] M. Michel B. Stewart A. Nesbitt D. Hepburn D. Guo C. Zhou, X. Zhou, "Comparison of digital filter, matched filter and wavelet transform in pd detection", International Council on Large Electric System (CIGRE), August session 2006.

[13] X. Song C. Zhou, D. M. Hepburn and M. Michel, "Application of denoising techniques to pd measurement utilising UHF, HFCT, acoustic sensors and IEC 60270", 20th International Conference and Exhibition on Electricity Distribution, June 2009.

[14] M. Florkowski and B. Florkowska, "Wavelet-based partial discharge image denoising", IET Generation, transmission, distribution, vol. 1, (2):344-347, March 2007.

[15] G. C. Montanari and A. Cavallini, F. Puletti: "A New Approach to Partial Discharge Testing of HV Cable Systems". IEEE Electrical Insulation Magazine, Vol. 22, No. 1, January/February 2006.

[16] X. Ma, C. Zhou, and I. Kemp, "Automated wavelet selection and thresholding for PO detection", IEEE Electrical Insulation Magazine, Vol. 18, No.2, pp. 37-45, 2002.

[17] IEC 60034-27: Off-line partial discharge measurements on the stator winding insulation of rotating electrical machines.

[18] IEC 60034-27-2: On-line partial discharge measurements on the stator winding insulation of rotating electrical machines. (Draft Standard)

[19] G.C. Stone, E.A. Boulter, I. Culbert, H. Dhirani, "Electrical Insulation for Rotating Machines", Wiley - IEEE Press, Jan. 2004.

Appendix A

Principle Appearance of PRPD Patterns

As per [17], different discharges have different types of PRPD pattern. These patterns can be used for comparison purposes and thus to find the PD source.

End-winding discharges: Fig. A.1 shows the PRPD pattern of surface discharges/tracking along the winding overhang due to contamination at the air/insulation interface

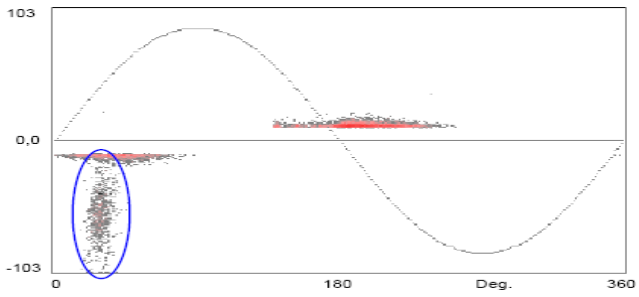

Figure A.1: PRPD Pattern of End-winding discharges

End-winding discharges: Fig. A.2 shows the PRPD pattern of discharges at the junction of the conductive slot coating and the stress control coating due to inadequate interface properties

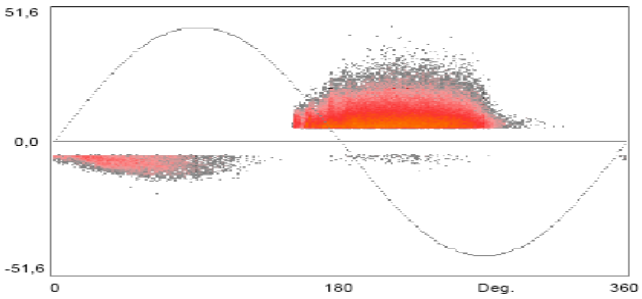

Figure A.2: PRPD Pattern of End-winding discharges

End-winding discharges: PRPD pattern of gap type discharges, between bars in the winding overhang or between a bar and the press finger of the core, is as shown in Fig. A.3

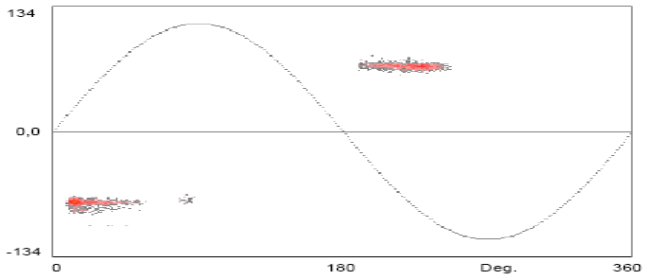

Figure A.3: PRPD Pattern of End-winding discharges

Internal void discharges: Fig. A.4 shows PRPD pattern for discharges from internal voids within the main insulation

Delamination discharges: Fig. A.5 shows PRPD pattern for discharges from delamination between the main insulation and the copper conductor

Slot discharges: Fig. A.6 shows PRPD pattern for slot discharges in the air gap between the laminated stator core and the side of the stator bar

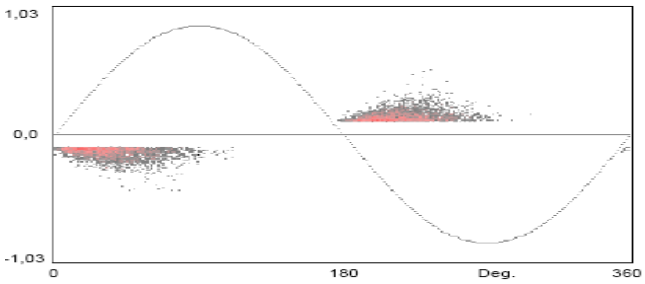

Figure A.4: PRPD Pattern of Internal Void discharges

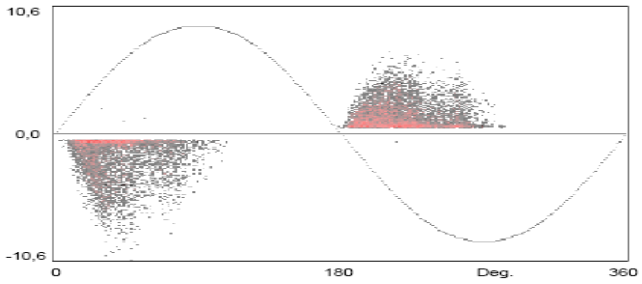

Figure A.5: PRPD Pattern of Delamination discharges

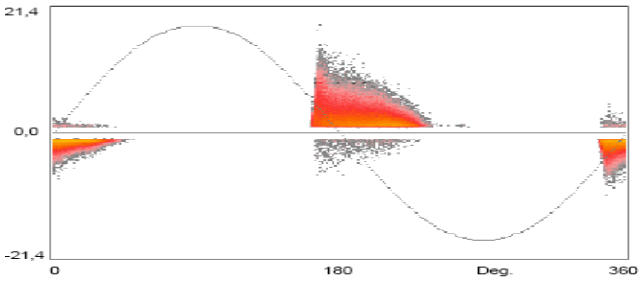

Figure A.6: PRPD Pattern of Slot discharges